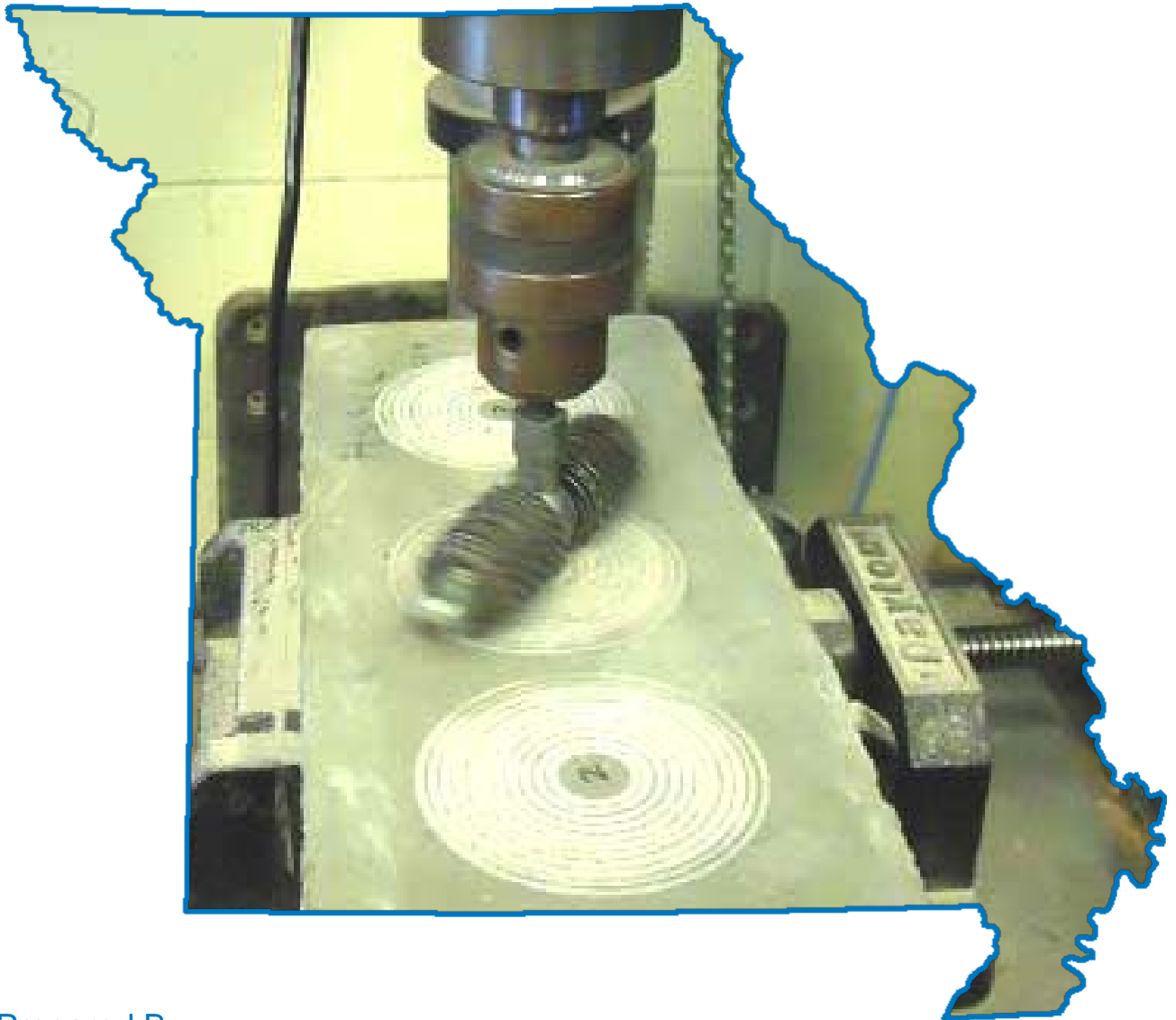


Self-Consolidating Concrete (SCC) for Infrastructure Elements Report D – Creep, Shrinkage and Abrasion Resistance



Prepared By:



MISSOURI UNIVERSITY OF SCIENCE AND TECHNOLOGY



Final Report Prepared for Missouri Department of Transportation
2012 August

Project TRyy1103

Report cmr 13-003

FINAL Report D

TRyy1103

Project Title: Self-Consolidating Concrete (SCC) for Infrastructure Elements

Report D: Self-Consolidating Concrete (SCC) for Infrastructure Elements: Creep, Shrinkage and Abrasion Resistance

Prepared for
Missouri Department of Transportation
Construction and Materials

Missouri University of Science and Technology, Rolla, Missouri

July 2012

The opinions, findings, and conclusions expressed in this publication are those of the principal investigators and the Missouri Department of Transportation. They are not necessarily those of the U.S. Department of Transportation, Federal Highway Administration. This report does not constitute a standard or regulation

ABSTRACT

Concrete specimens were fabricated for shrinkage, creep, and abrasion resistance testing. Variations of self-consolidating concrete (SCC) and conventional concrete were all tested. The results were compared to previous similar testing programs and used to determine the adequacy of the materials for use in practice.

The testing program consisted of normal strength (6000 psi) and high strength (10,000 psi) variations of SCC and conventional concrete.

All specimens were tested for compressive strength, modulus of elasticity, shrinkage strain, creep strain, and abrasion resistance. All tests were performed according to their respective ASTM standard methods. In general, SCC performed well relative to conventional concrete at high strengths, but not as well at normal strengths for shrinkage and creep.

TABLE OF CONTENTS

	Page
ABSTRACT	iii
LIST OF ILLUSTRATIONS	vii
LIST OF TABLES	ix
NOMENCLATURE	x
1. LITERATURE REVIEW	1
SECTION	
1.1. SELF-CONSOLIDATING CONCRETE (SCC)	1
1.1.1. Definition of SCC	1
1.1.2. Advantages of SCC	1
1.2. SHRINKAGE OF CONCRETE	1
1.2.1. Definition of Shrinkage	1
1.2.2. Factors Affecting Shrinkage	2
1.3. SHRINKAGE MODELS	4
1.3.1. ACI 209R-92	4
1.3.2. NCHRP Report 496 (2003)	8
1.3.3. Model B3	10
1.3.4. CEB-FIP 90	11
1.3.5. GL 2000	12
1.4. SCC SHRINKAGE RESEARCH	13
1.4.1. NCHRP Report 628 (2009)	14
1.4.2. Shindler, et. al.	14
1.4.3. Fernandez-Gomez and Landsberger	15
1.4.4. Long, et. al.	15
1.5. CREEP OF CONCRETE	16
1.5.1. Definition of Creep	16
1.5.2. Factors Affecting Creep	17
1.6. CREEP MODELS	18
1.6.1. ACI 209R-92	18

1.6.2. NCHRP Report 496.....	20
1.6.3. CEB-FIP 90	21
1.6.4. GL 2000.....	22
1.7. SCC CREEP RESEARCH.....	23
1.7.1. NCHRP Report 628.....	23
1.7.2. Long and Khayat	24
1.7.3. Long, et. el.....	24
1.8. Application of Shrinkage and Creep.....	24
1.8.1. Prestress Loss	24
1.8.2. Load Effects	26
1.8.3. Beam Deflection.....	26
1.9. CONCRETE ABRASION	27
1.9.1. Definition of Concrete Abrasion	27
1.9.2. Factors Affecting Concrete Abrasion.....	27
1.10. SCC ABRASION RESEARCH.....	27
2. RESEARCH PROGRAM	28
2.1. MIX DESIGNS.....	28
2.1.1. SCC..	28
2.2. SHRINKAGE AND CREEP SPECIMEN CONSTRUCTION.....	29
2.2.1. Shrinkage and Creep Specimens	29
2.2.2. Shrinkage and Creep Molds	30
2.2.3. Shrinkage and Creep Specimen Casting	31
2.2.4. Shrinkage and Creep De-Molding and Preparation	31
2.2.5. Shrinkage and Creep Data Acquisition	31
2.3. ABRASION SPECIMEN CONSTRUCTION	32
2.4. TESTING PROCEDURES.....	33
2.4.1. Shrinkage Testing Procedures	33
2.4.2. Creep Testing Procedures.....	36
2.4.3. Abrasion Resistance Testing Procedures	39
3. SCC RESULTS AND DISCUSSION.....	43
3.1. SHRINKAGE	43

3.1.1. Results	43
3.1.2. Discussion and Conclusions	43
3.2. CREEP	52
3.2.1. Results	52
3.2.2. Discussion and Conclusions	53
3.3. ABRASION RESISTANCE	57
3.3.1. Results	57
3.3.2. Discussion and Conclusions	60
APPENDICES	
A. SHRINKAGE WITH RELATIVE HUMIDITY DATA	62
B. EXAMPLE STRAIN CALCULATIONS	67
C. COEFFICIENT OF VARIATION DATA	70
BIBLIOGRAPHY	73

LIST OF ILLUSTRATIONS

Figure	Page
Figure 1.1 - Relationship Between Moist Cure Time and Shrinkage Strain	3
Figure 1.2 - Stress vs. Time for Prestressed Bridge Girder (Tadros et. al. 2003).....	25
Figure 2.1 - Shrinkage and Creep Form.....	30
Figure 2.2 – Shrinkage and Creep Specimens and DEMEC Point Arrangement (Myers and Yang, 2005).....	32
Figure 2.3 – DEMEC Reading Taken on Specimen.....	34
Figure 2.4 - Reference Bar.....	34
Figure 2.5 - Reading Taken on Reference Bar	35
Figure 2.6 - Gauge Factor Used for Shrinkage and Creep Calculations.....	35
Figure 2.7 - Example DEMEC Gauge Reading.....	35
Figure 2.8 - Schematic of Creep Loading Frame (Myers and Yang, 2005)	36
Figure 2.9 - Creep Loading Frame with Specimen.....	37
Figure 2.10 - Reading Taken on Creep Specimen	38
Figure 2.11 - Schematic of Abrasion Rotating Cutter (ASTM C944).....	40
Figure 2.12 - Rotating Cutter	40
Figure 2.13 - Abrasion Resistance Test In Progress.....	41
Figure 2.14 - Depth of Wear Measurement Points	41
Figure 2.15 - Abrasion Resistance Specimen After Testing.....	42
Figure 3.1 - C6-58L Shrinkage Results and Prediction Models	46
Figure 3.2 - S6-48L Shrinkage Results and Prediction Models.....	47
Figure 3.3 - C10-58L Shrinkage Results and Prediction Models	48
Figure 3.4 - S10-58L Shrinkage Results and Prediction Models.....	49
Figure 3.5 - SCC Shrinkage Results (Best fit Logarithmic).....	50
Figure 3.6 – SCC Results with Shrinkage Databases (Fernandez-Gomez, Shindler et. al., and Holshemacher).....	51
Figure 3.7 – SCC Coefficient of Creep Results.....	54
Figure 3.8 – S6-48L Plotted Against Results from Long and Khayat (2011)	55
Figure 3.9 – S10-48L Plotted Against Results from Long and Khayat (2011)	56

Figure 3.10 - C6-58L Mass Loss Results.....	57
Figure 3.11 - S6-48L Mass Loss Results	58
Figure 3.12 - C10-58L Mass Loss Results.....	58
Figure 3.13 - S10-48L Mass Loss Results	59
Figure 3.14 - SCC Mass Loss Results	59
Figure 3.15 - SCC Depth of Wear Results.....	60
Figure A.1 – C6-58L shrinkage data shown with recorded relative humidity.....	63
Figure A.2 - S6-48L shrinkage data shown with recorded relative humidity.....	64
Figure A.3 – C10-58L shrinkage data shown with recorded relative humidity.....	65
Figure A.4 – S10-48L shrinkage data shown with recorded relative humidity	66
Figure B.1 – Example shrinkage and creep strain calculation.....	68
Figure B.2 – Example shrinkage and creep strain calculations with equations shown	69
Figure C.1 – C6-58L and S6-48L COV Data	71
Figure C.2 – C10-58L and S10-48L COV Data	72

LIST OF TABLES

Table	Page
Table 1.1 - Standard Conditions as Defined by ACI 209R-92	6
Table 1.2 – Coded Values for Eqs. 1.48 – 1.49	16
Table 2.1 - SCC Test Program Mix Designs and mechanical properties	29
Table 3.1 – SCC results compared to Eqs. 2.48 – 2.49 by Long et. al.	52
Table 3.2 - Summary of SCC Creep Results	52
Table 3.3 - Summary of Results Shown with 28 Day Measured Compressive Strength .	60

NOMENCLATURE

Symbol	Description
A	Cement type correction factor (NCHRP 628)
A_c	Cross-section area (mm^2) (CEB-FIP 90)
c	Cement content (lb/yd^3) (ACI 209R-92)
D	Effective cross-section thickness (Model B3)
D_0	Datum reading on the reference bar
D_i	Subsequent reading on the reference bar
f	Size effects factor (ACI 209R-92)
f'_c	Tested compressive strength of concrete (psi, ksi, MPa)
f'_{ci}	Specified compressive strength of concrete (ksi) (NCHRP 496)
f_{cm}	Tested compressive strength of concrete at 28 days age (psi, ksi, MPa) (CEB-FIP 90)
G	Gauge factor
H	Relative humidity (% or decimal)
K	Cement type correction factor (GL 2000)
k_f	Concrete strength factor (NCHRP 496)
k_{hc}	Humidity factor (NCHRP 496)
k_{hs}	Humidity factor (NCHRP 496 and NCHRP 628)
k_{la}	Loading factor (NCHRP 496)
k_s	Size factor (NCHRP 496 and NCHRP 628) or Cross-section shape factor (Model B3)
k_{td}	Time development factor (NCHRP 496)

R_0	Datum reading on tested material
RH	Relative humidity (%) (CEB-FIP 90)
R_i	Subsequent reading on tested material
s	Slump of fresh concrete (in)
S(t)	Time dependence factor (Model B3)
t	Age of concrete (days)
t_0	Age of concrete when drying begins (days) (Model B3) or Age at which creep specimen is loaded (days) (ACI 209R-92 and CEB FIP 90)
t_c	Age of concrete when drying begins (days) (ACI 209R-92 and GL 2000)
t_i	Age at which creep specimen is loaded (days) (NCHRP 496)
t_s	Age of concrete at the beginning of shrinkage (days) (CEB-FIP 90)
u	Perimeter in contact with the atmosphere (mm) (CEB-FIP 90)
V/S	Volume to Surface area ratio (in or mm)
w	Water content of concrete (lb/ft ³)
α	Concrete air content (%)
α_1	Cement type correction factor (Model B3)
α_2	Curing condition correction factor
$\beta(h)$	Humidity correction factor (GL 2000)
$\beta(t)$	Time effect correction factor (GL 2000)
β_c	Coefficient to describe the development of creep with time after loading (CEB FIP 90)

β_{RH}	Relative humidity correction factor (CEB-FIP 90)
β_s	Coefficient to describe the development of shrinkage with time (CEB-FIP 90)
β_{sc}	Concrete type correction factor (CEB-FIP 90)
$\gamma_{c,RH}$	Humidity correction factor (ACI 209R-92)
$\gamma_{c,s}$	Slump correction factor (ACI 209R-92)
$\gamma_{c,t0}$	Curing condition correction factor (ACI 209R-92)
$\gamma_{c,vs}$	Size correction factor (ACI 209R-92)
$\gamma_{c,\alpha}$	Air content correction factor (ACI 209R-92)
$\gamma_{c,\psi}$	Fine aggregate correction factor (ACI 209R-92)
$\gamma_{sh,c}$	Cement content correction factor (ACI 209R-92)
$\gamma_{sh,RH}$	Relative humidity correction factor (ACI 209R-92)
$\gamma_{sh,s}$	Slump correction factor (ACI 209R-92)
$\gamma_{sh,tc}$	Initial moist cure duration correction factor (ACI 209R-92)
$sh_{,vs}$	Volume/surface area correction factor (ACI 209R-92)
$\gamma_{sh,\alpha}$	Air content correction factor (ACI 209R-92)
$\gamma_{sh,\psi}$	Fine aggregate correction factor (ACI 209R-92)
$\Delta_{\epsilon c}$	Change in creep strain from one reading to the next
$\Delta_{\epsilon s}$	Change in shrinkage strain from one reading to the next
ϵ_{cso}	Notional shrinkage coefficient (CEB-FIP 90)
$\epsilon_{es(t,ts)}$	Calculated ultimate shrinkage strain ($\mu\epsilon$) (CEB-FIP 90)
ϵ_i	Measured strain due to initial loading of creep specimen
$\epsilon_{es(t,t0)}$	Calculated shrinkage strain at a given age ($\mu\epsilon$) (Model B3)

ϵ_{sh}	Calculated shrinkage strain at a given age ($\mu\epsilon$) (NCHRP 496, GL 2000, and NCHRP 628)
$\epsilon_{sh(t,tc)}$	Calculated shrinkage strain at a given age ($\mu\epsilon$) (ACI 209R-92)
ϵ_{shu}	Calculated ultimate shrinkage strain ($\mu\epsilon$) (ACI 209R-92) or Notional ultimate shrinkage strain (GL 2000)
$\epsilon_{sh\infty}$	Calculated ultimate shrinkage strain ($\mu\epsilon$) (Model B3)
ϵ_t	Measured creep strain at a given age
λ_{Δ}	Multiplier for additional deflection due to long-term effects (ACI 318-08)
ξ	Time dependant factor for sustained load (ACI 318-08)
ρ'	Compression reinforcement ratio (ACI 318-08)
τ_{sh}	Size dependence factor (Model B3)
$\Phi_{(t,t_0)}$	Calculated creep coefficient at a given age (ACI 209R-92 and CEB FIP 90) or Measured creep coefficient at a given age
Φ_0	Notional creep coefficient (CEB FIP 90)
Φ_{28}	Calculated creep coefficient at a given age (GL 2000)
$\Phi_{(tc)}$	Factor that takes into account drying before loading (GL 2000)
Φ_u	Calculated ultimate creep coefficient (ACI 209R-92)
Ψ	Ratio of fine aggregate to total aggregate by weight (%)
$\Psi_{(t,t_i)}$	Calculated creep coefficient at a given age (NCHRP 496 and NCHRP 628)

1. LITERATURE REVIEW

1.1. SELF-CONSOLIDATING CONCRETE (SCC)

1.1.1. Definition of SCC. ACI 237R-07 defines self-consolidating concrete as “highly flowable, nonsegregating concrete that can spread into place, fill the formwork, and encapsulate the reinforcement without any mechanical consolidation.” In order to achieve the necessary fluidity, a high range water reducer (HRWR) is often utilized.

1.1.2. Advantages of SCC. The choice of SCC over conventional concrete results in both economical and material performance benefits. The use of SCC eliminates the necessity of manual compaction, typically achieved by vibration. The self-leveling properties of SCC additionally reduce or eliminate the need for screeding operations to achieve a flat surface. This reduction in jobsite labor and equipment forces, along with the time saved by not having to perform these labor intensive operations, lead to significant savings. Because of its fluidity, SCC has the ability to effectively flow into areas that conventional concrete cannot. SCC is therefore ideal for construction of members with significant reinforcement congestion or unusually shaped members. This allows for greater freedom in member design and reinforcement detailing. Finally, the reduction in honeycombing is beneficial both structurally and aesthetically (ACI 237R-07).

1.2. SHRINKAGE OF CONCRETE

1.2.1. Definition of Shrinkage. Shrinkage of concrete is the decrease in volume of hardened concrete with time. Shrinkage is expressed as the strain measured on a load-free specimen, most often as the dimensionless unit microstrain (strain $\times 10^{-6}$).

Concrete experiences shrinkage in three ways, drying shrinkage, autogenous (chemical) shrinkage, and carbonation shrinkage. Autogenous shrinkage is due strictly to the hydration reactions of the cement. Drying shrinkage is the strain imposed on a specimen exposed to the atmosphere and allowed to dry. Carbonation shrinkage is caused by the reaction of calcium hydroxide with cement with carbon dioxide in the atmosphere. The magnitude and rate of shrinkage is dependent on a number of factors. These factors are accounted for and described in the various industry models and research projects in the following sections.

1.2.2. Factors Affecting Shrinkage (ACI 209.1R-05). Shrinkage of concrete is closely related to shrinkage of paste. Therefore the amount of paste in the mix significantly affects the level of concrete shrinkage. Paste volume is determined by the quantity, size, and gradation of aggregate. Because paste volume is largely dependent on aggregate properties, the most important factor in determining a concrete's shrinkage level is the aggregate used in the mix. Similarly, the water content, cement content, and slump will affect the shrinkage of concrete. These three factors are indications of the paste volume and therefore can be used to determine the shrinkage potential of a mix. Aggregate acts as a restraining force to shrinkage, therefore an aggregate with a higher modulus of elasticity (MOE) will better restrain against shrinkage than an aggregate with a lower MOE. The characteristics of the cement itself are other significant indicators of shrinkage potential. Research has shown cements with low sulfate content, high alumina content, and cements that are finely ground exhibit increased shrinkage.

The environment which the concrete is exposed to can also influence shrinkage. The biggest environmental factor is the relative humidity of the surrounding air. As

shown by **Eq. 1.1**, as relative humidity increases, shrinkage decreases due to the decrease in potential moisture loss. It has also been shown that an increase in temperature increases the ultimate shrinkage of concrete.

$$\text{shrinkage} \propto 1 - \left(\frac{h}{100}\right)^b \quad (1.1)$$

Where: h is relative humidity in percent, and b is a constant that ranges from 1 to 4.

Finally, the design and construction of concrete specimens can influence shrinkage. The curing conditions experienced by the concrete have a significant effect on shrinkage.

Generally, the longer the specimen is allowed to moist cure, the less it will shrink.

However, research conducted by Perenchio (1997), **Figure 1.1**, shows that there may not be a simple relationship between moist cure time and shrinkage.

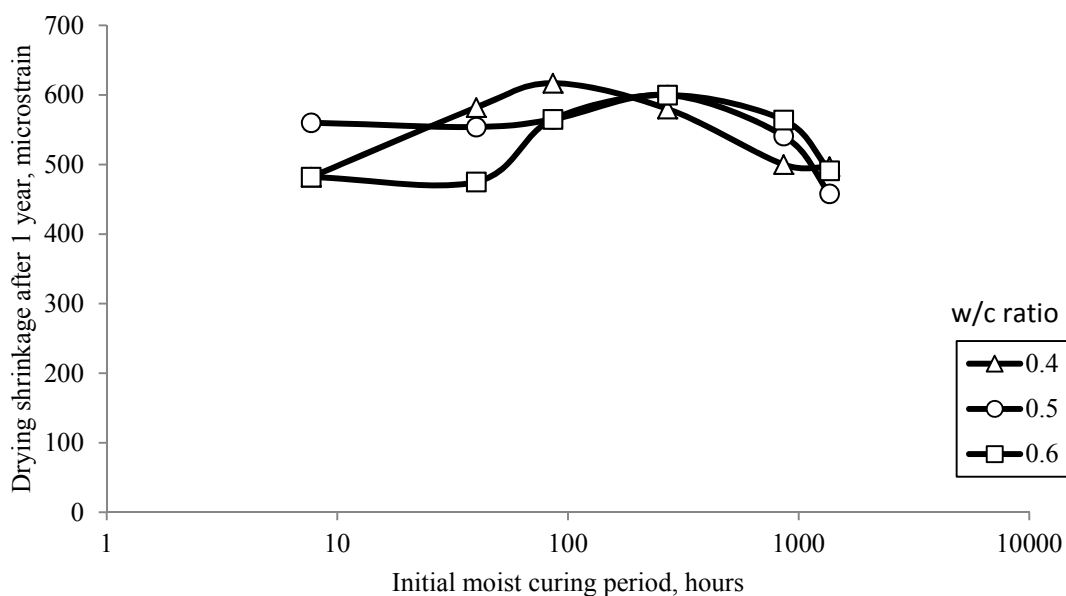


Figure 1.1 - Relationship Between Moist Cure Time and Shrinkage Strain

(adapted from Perenchio 1997)

Larger members tend to dry slower, so the ratio of volume to surface area is a significant factor in shrinkage of concrete.

$$\text{shrinkage} \propto \frac{1}{\left(\frac{V}{S}\right)^2} \quad (1.2)$$

Where: V/S is the volume to surface area ratio in inches.

1.3. SHRINKAGE MODELS.

The ability to accurately predict the shrinkage of a concrete structure is extremely important. An accurate model for shrinkage will allow the engineer to predict long term serviceability, durability, and stability of a given structure. As mentioned above, there are many different factors that affect a concrete's susceptibility to shrinkage. Because of these factors, accurate prediction of shrinkage is very difficult. The models described below take into account many of the factors described above in their attempt to predict concrete shrinkage (Bazant and Baweja, 2000).

1.3.1. ACI 209R-92. This model, developed by Branson and Christiason (1971) and modified by ACI committee 209, predicts shrinkage strain of concrete at a given age under standard conditions. The original model by Branson and Christiason was developed based on a best fit from a sample of 95 shrinkage specimens and using an ultimate shrinkage strain of 800×10^{-6} in./in. (mm/mm). However, subsequent research by Branson and Chen, based on a sample of 356 shrinkage data points, concluded that the

ultimate shrinkage strain should be 780×10^{-6} in./in. (mm/mm). The prediction model, **Eq. 1.3 – 1.5**, apply only to the standard conditions as shown in **Table 1.1**.

$$\epsilon_{sh}(t, t_c) = \frac{(t-t_c)^\alpha}{f+(t-t_c)^\alpha} \epsilon_{shu} \quad (\mu\epsilon) \quad (1.3)$$

$$\epsilon_{shu} = 780 \times 10^{-6} \quad (\mu\epsilon) \quad (1.4)$$

$$f = 26.0e^{\{0.36(V/S)\}} \quad (1.5)$$

Where: f is 35 (moist cure) or 55 (steam cure), or by **Eq. 1.5** if size effects are to be considered, α is assumed to be 1, t is the age of concrete in days, and t_c is the age of concrete when drying begins in days.

Table 1.1 - Standard Conditions as Defined by ACI 209R-92

Factors		Variables		Standard
Concrete	Concrete Composition	Cement Paste Content	Type of Cement	Type I or III
		W/C	Slump	2.7 in (70mm)
		Mix Proportions	Air Content	≤ 6%
		Aggregate Characteristics	Fine Aggregate %	50%
		Degree of Compaction	Cement Content	470 to 752 lb/yd ³ (279 to 446 kg/m ³)
	Initial Curing	Length of Initial Curing	Moist Cured	7 days
			Steam Cured	1 - 3 days
		Curing Temperature	Moist Cured	73.4 ± 4°F (23 ± 2°C)
			Steam Cured	≤ 212°F (≤ 100°C)
		Curing Humidity	Relative Humidity	≥ 95%
Member Geometry & Environment	Environment	Concrete Temperature	Concrete Temperature	73.4°F ± 4°F (23 ± 2°C)
		Concrete Water Content	Ambient Relative Humidity	40%
	Geometry	Size and Shape	Volume-Surface Ratio (V/S)	V/S = 1.5 in (38mm)
			Minimum Thickness	6 in (150mm)

When concrete is not subject to any or all of the standard conditions, correction factors shall be applied, as shown in **Eq. 1.6 – 1.16**.

$$\epsilon_{sh}(t, t_c) = \frac{(t-t_c)^\alpha}{f+(t-t_c)^\alpha} \times \epsilon_{shu} \quad (\mu\epsilon) \quad (1.6)$$

$$f = 26.0e^{\{0.36(V/S)\}} \quad (1.7)$$

$$\epsilon_{shu} = 780\gamma_{sh} \times 10^{-6} \quad (\mu\epsilon) \quad (1.8)$$

$$\gamma_{sh} = \gamma_{sh,tc} \gamma_{sh,RH} \gamma_{sh,vs} \gamma_{sh,s} \gamma_{sh,\psi} \gamma_{sh,c} \gamma_{sh,\alpha} \quad (1.9)$$

$$\gamma_{sh,tc} = 1.202 - .2337 \log(t_c) \quad (1.10)$$

$$\gamma_{sh,RH} = \begin{cases} 1.40 - 1.02h & \text{for } 0.40 \leq h \leq 0.80 \\ 3.00 - 3.0h & \text{for } 0.80 \leq h \leq 1 \end{cases} \quad (1.11)$$

$$\gamma_{sh,vs} = 1.2e^{\{-0.12(V/S)\}} \quad (1.12)$$

$$\gamma_{sh,s} = 0.89 + 0.041s \quad (1.13)$$

$$\gamma_{sh,\psi} = \begin{cases} 0.30 + 0.014\psi & \text{for } \psi \leq 50\% \\ 0.90 + 0.002\psi & \text{for } \psi > 50\% \end{cases} \quad (1.14)$$

$$\gamma_{sh,c} = 0.75 + 0.00036c \quad (1.15)$$

$$\gamma_{sh,\alpha} = 0.95 + 0.008\alpha \geq 1 \quad (1.16)$$

Where: $\epsilon_{sh}(t, t_c)$ is the calculated shrinkage strain at a given age, ϵ_{shu} is the calculated ultimate shrinkage strain, $\gamma_{sh,tc}$ is the initial moist cure duration correction factor, t is the age of concrete in days, t_c is the age of concrete when drying starts in days, $\gamma_{sh,RH}$ is the

relative humidity correction factor, h is humidity in decimals, $\gamma_{sh,vs}$ is the volume/surface area correction factor, where V/S is the volume to surface area ratio in inches, $\gamma_{sh,s}$ is the slump correction factor, s is slump in inches, $\gamma_{sh,\psi}$ is the fine aggregate correction factor, ψ is the ratio of fine aggregate to total aggregate by weight expressed as percentage, $\gamma_{sh,c}$ is the cement content correction factor, c is the cement content in lb/yd^3 , $\gamma_{sh,\alpha}$ is the air content correction factor, and α is the air content in percent. In **Eq 1.6**, the value of α can be assumed to be equal to 1, with f assumed to be equal to 35 for concrete that is moist cured for seven days or 55 for concrete subject to 1-3 days of steam curing. In order to totally consider shape and size effects, α is still assumed to be equal to 1, with f given by **Eq. 1.7**.

1.3.2. NCHRP Report 496 (2003). The National Cooperative Highway Research Program (NCHRP) conducted research on shrinkage of high strength concrete in the states of Nebraska, New Hampshire, Texas, and Washington. This research project was sponsored by the American Association of State Highway and Transportation Officials (AASHTO) and the results adopted into the 2007 AASHTO LRFD Bridge Design Specifications. Laboratory shrinkage data was obtained from three 4 in. (101.6 mm) by 4 in. (101.6 mm) by 24 in. (609.6 mm) specimens per mix, with a total of 48 specimens tested including both normal and high strength concrete. Field specimens were also made and cured in the same condition as corresponding bridge girders in each of the four participating states. The field program consisted of a set of three 4 in. (101.6 mm) by 4 in. (101.6 mm) by 24 in. (609.6 mm) shrinkage specimens at each location with measurements taken for 3 months. The data showed that an ultimate shrinkage strain of 480×10^{-6} in./in. (mm/mm) should be assumed. The modification factors in the model

account for the effects of high strength concrete. **Eq. 1.17 – 1.22** present the proposed shrinkage formula as proposed in this study.

$$\varepsilon_{sh} = 480 \times 10^{-6} \gamma_{sh} \quad (\mu\varepsilon) \quad (1.17)$$

$$\gamma_{sh} = k_{td} k_s k_{hs} k_f \quad (1.18)$$

$$k_{td} = \frac{t}{61 - 4f'_{ci} + t} \quad (1.19)$$

$$k_{hs} = 2.00 - 0.0143H \quad (1.20)$$

$$k_s = \frac{1064 - 94V/S}{735} \quad (1.21)$$

$$k_f = \frac{5}{1 + f'_{ci}} \quad (1.22)$$

Where: ε_{sh} is the calculated shrinkage strain at a given age, k_{td} is the time development factor, t is the age of the concrete in days, k_{hs} is the humidity factor, H is the average ambient relative humidity in percent, k_s is the size factor, V/S is the volume to surface area ratio in inches, k_f is the concrete strength factor, and f'_{ci} is the specified compressive strength of concrete in ksi.

1.3.3. Model B3. Model B3 (Bazant and Baweja) is the third update of shrinkage predictions developed at Northwestern University, based on BP model β_3 and BP-KX model β_4 . This model is simpler than previous versions and is validated by a larger set of test data. **Eq. 1.23 – 1.32** present the B3 shrinkage prediction model.

$$\varepsilon_{sh}(t, t_0) = -\varepsilon_{sh\infty} k_h S(t) \quad (\mu\varepsilon) \quad (1.23)$$

$$S(t) = \tanh \sqrt{\frac{t-t_0}{\tau_{sh}}} \quad (1.24)$$

$$k_h = \begin{cases} 1 - h^3 & \text{for } h \leq 0.98 \\ -0.2 & \text{for } h = 1 \text{ (swelling in water)} \\ \text{linear} & \\ \text{interpolation} & \text{for } 0.98 \leq h \leq 1 \end{cases} \quad (1.25)$$

$$\tau_{sh} = k_t (k_s D)^2 \quad (1.26)$$

$$k_t = 190.8 t_0^{-0.08} f'_c{}^{-1/4} \quad (1.27)$$

$$D = 2V/S \text{ (in.)} \quad (1.28)$$

$$k_s = \begin{cases} 1.00 & \text{for an infinite slab} \\ 1.15 & \text{for an infinite cylinder} \\ 1.25 & \text{for an infinite square prism} \\ 1.30 & \text{for a sphere} \\ 1.55 & \text{for a cube} \end{cases} \quad (1.29)$$

$$\varepsilon_{sh\infty} = -\alpha_1\alpha_2[26w^{2.1}f'_c{}^{-0.28} + 270] \quad (\mu\varepsilon) \quad (1.30)$$

$$\alpha_1 = \begin{array}{ll} 1.0 & \text{for type I cement} \\ 0.85 & \text{for type II cement} \\ 1.1 & \text{for type III cement} \end{array} \quad (1.31)$$

$$\alpha_2 = \begin{array}{ll} 0.75 & \text{for steam – curing} \\ 1.2 & \text{for sealed or normal curing in air} \\ & \text{with initial protection against drying} \\ 1.0 & \text{for curing in water or at 100\% relative humidity} \end{array} \quad (1.32)$$

Where: $\varepsilon_{shu}(t, t_0)$ is the calculated shrinkage strain at a given age, $S(t)$ is the time dependence factor, t is the age of concrete in days, t_0 is the age of concrete at which drying begins, τ_{sh} is the size dependence factor, f'_c is the cylinder compressive strength in psi, D is the effective cross-section thickness, V/S is the volume to surface area ratio in inches, k_s is the cross-section shape factor, $\varepsilon_{sh\infty}$ is the calculated ultimate shrinkage strain, α_1 is the cement type correction factor, α_2 is the curing condition correction factor, and w is the water content of the concrete in lb/ft^3 .

1.3.4. CEB-FIP 90. This model, developed jointly by Euro-International Concrete Committee (CEB – Comité Euro-International du Béton) and the International Federation for Prestressing (FIP – Fédération Internationale de la Précontrainte) is found in the CEB-FIP Model Code 1990. It is stated that due to its international character, the code is more general than most and does not apply to any particular structure type. **Eq. 1.33 – 1.38** present this model for calculating shrinkage strain.

$$\varepsilon_{es}(t, t_s) = \varepsilon_{cso}\beta_s(t - t_s) \quad (\mu\varepsilon) \quad (1.33)$$

$$\varepsilon_{\text{cso}} = \varepsilon_s(f_{\text{cm}})(\beta_{\text{RH}}) \quad (1.34)$$

$$\beta_s(t - t_s) = \sqrt{\frac{(t - t_s)}{350 \left(\frac{2A_c}{100u} \right)^2 + (t - t_s)}} \quad (1.35)$$

$$\varepsilon_s(f_{\text{cm}}) = [160 + 10\beta_{\text{sc}}(9 - 0.1f_{\text{cm}})] \times 10^{-6} \quad (1.36)$$

$$\beta_{\text{RH}} = -1.55 \left[1 - \left(\frac{\text{RH}}{100} \right)^3 \right] \quad (1.37)$$

$$\beta_{\text{sc}} = \begin{cases} 4 & \text{for slowly hardening cements} \\ 5 & \text{for normal or rapid hardening cements} \\ 8 & \text{for rapid hardening high strength cements} \end{cases} \quad (1.38)$$

Where: $\varepsilon_{\text{es}}(t, t_s)$ is the calculated ultimate shrinkage strain, ε_{cso} is the notional shrinkage coefficient, β_s is the coefficient to describe the development of shrinkage with time, t is the age of concrete in days, t_s is the age of concrete at the beginning of shrinkage in days, A_c is the cross section area in mm^2 , u is the perimeter in contact with the atmosphere in mm, f_{cm} is the compressive strength of concrete at age of 28 days in MPa, β_{RH} is the relative humidity correction factor, RH is the relative humidity in percent, and β_{sc} is the concrete type correction factor.

1.3.5. GL 2000. This model, developed by Gardener and Lockman was published in the ACI materials journal under the title “Design provisions for drying shrinkage and Creep of Normal-Strength Concrete.” The model developed is shown in **Eq. 1.39 – 1.43.**

$$\varepsilon_{sh} = \varepsilon_{shu}\beta(h)\beta(t) \quad (\mu\varepsilon) \quad (1.39)$$

$$\varepsilon_{shu} = 1000K\sqrt{\frac{30}{f'_c}} \times 10^{-6} \quad (\mu\varepsilon) \quad (1.40)$$

$$\beta(h) = 1 - 1.18h^4 \quad (1.41)$$

$$\beta(t) = \sqrt{\frac{t-t_c}{t-t_c+0.15(V/S)^2}} \quad (1.42)$$

$$K = \begin{array}{ll} 1 & \text{for type I cement} \\ 0.75 & \text{for type II cement} \\ 1.15 & \text{for type III cement} \end{array} \quad (1.43)$$

Where: ε_{sh} is the calculated shrinkage strain at a given age, ε_{shu} is the notional ultimate shrinkage strain, $\beta(h)$ is the humidity correction factor, h is humidity in decimals, $\beta(t)$ is the correction factor for the effect of time on shrinkage, t_c is the age that drying has commenced in days, t is age of concrete in days, V/S is the volume to surface area ratio, and K is the cement type correction factor.

1.4. SCC SHRINKAGE RESEARCH

A number of shrinkage models have been developed which are formulated specifically for self consolidating concrete. The sections to follow present some shrinkage models that apply to SCC.

1.4.1. NCHRP Report 628 (2009). The study undertaken as part of NCHRP Report 628 concluded that the most accurate current prediction model for shrinkage of SCC was the CEB-FIP 90 at the time of investigation. Following the comparison of test data to available models, the NCHRP study also proposed a shrinkage model for SCC. This model, shown in **Eq. 1.44 – 1.47**, is simply the AASHTO 2004 prediction model with an added calibration factor, A , which accounts for effects of SCC.

$$\epsilon_{sh} = -k_s k_{hs} \left(\frac{t}{55+t} \right) 0.56 \times 10^{-3} \times A \quad (\mu\epsilon) \quad (1.44)$$

$$k_{hs} = 2.00 - 0.0143H \quad (1.45)$$

$$k_s = \left[\frac{\frac{t}{26e^{0.0142(V/S)+t}}}{\frac{t}{45+t}} \right] \left[\frac{1064-3.70(V/S)}{923} \right] \quad (1.46)$$

$$A = \begin{array}{ll} 0.918 & \text{for Type I/II cement} \\ 1.065 & \text{for Type III cement} \end{array} \quad (1.47)$$

Where: ϵ_{sh} is the calculated shrinkage strain at a given age, k_s is the size factor, k_{hs} is the humidity factor, H is relative humidity in percent, t is drying time in days, V/S is the volume to surface area ratio, and A is the cement type correction factor.

1.4.2. Shindler, et. al. The goal of this project was to investigate the shrinkage potential of typical mixes used in precast/prestressed concrete construction. Twenty-one SCC mixes were tested along with two conventional mixes. The specimens tested were 3 in. (76.2 mm) by 3 in. (76.2 mm) by 11.25 in. (285.75 mm) prisms. They

were cured in a lime bath for seven days prior to drying. The results suggest very little difference in 28 day shrinkage between the SCC and conventional mixes. At 112 days, the SCC mixes performed better on average than the conventional mixes.

1.4.3. Fernandez-Gomez and Landsberger. Experimental shrinkage results were gathered from 25 published investigations. The database compiled included results from 93 SCC mixes and 30 conventional concrete (CC) mixes. The results were analyzed in order to determine which shrinkage model best fit the data. The models analyzed were CEB-FIP 90, ACI 209, B3, GL 2000, and the Spanish EHE model. The Spanish EHE model is based on the CEB-FIP 90 model; however, it doesn't include the factor accounting for cement type. The data was also analyzed to determine which material or mix parameters most influenced shrinkage strain. It was concluded that, based on three statistical models (best-fit line, residual analysis, and coefficient of variation), the B3 and ACI 209 models best predicted shrinkage results for both SCC and CC.

1.4.4. Long, et. al. The goal of this study was to develop equations to predict mechanical properties, workability, and visco-elastic properties of SCC. This was accomplished by evaluating 16 different SCC mixes and determining the key parameters which effect the desired properties. The parameters evaluated were the binder content, binder type, w/c, viscosity modifying admixture (VMA) content, and sand to aggregate ratio (S/A). Using statistical analysis of the data obtained, the following equations were developed. The variables in the equations are defined according to **Table 1.2**.

Table 1.2 – Coded Values for Eqs. 1.48 – 1.49

Absolute	Coded		
	-1	0	+1
Binder content (BC) (kg/m ³)	440	470	500
Binder type (BT)	Type MS	Type MS + HE	Type HE + 20% FA
w/cm	0.34	0.37	0.40
VMA content (mL/100 kg CM)	0	50	100
Sand-to-aggregate ratio (S/A) By volume	0.46	0.50	0.54

Conversion: 1 kg/m³ = 1.686 lb/yd³
 1 mL/100kg = 1.707 fl. oz./100 lb.

56 day autogenous shrinkage:

$$\begin{aligned} \mu\varepsilon = & +201 + 67.1 BT - 40.6 w/cm - 18.8 (BC \cdot w/cm) \\ & +17.8 (BC \cdot S/A) \quad (\mu\varepsilon) \end{aligned} \quad (1.48)$$

112 day drying shrinkage:

$$\begin{aligned} \mu\varepsilon = & +554 - 58.1 w/cm + 48.4 BC + 46.2 (w/cm \cdot VMA) \\ & +41.9 (w/cm \cdot BT) - 40.6 (BC \cdot VMA) + 37.4 S/A \\ & +30.8 (VMA \cdot BT) \quad (\mu\varepsilon) \end{aligned} \quad (1.49)$$

1.5. CREEP OF CONCRETE

1.5.1. Definition of Creep. Creep of concrete is defined as “the time-dependent increase in strain under sustained constant load taking place after the initial strain at loading.” (ACI 209.1R-05). Initial strain is the short term strain at the moment of loading. Initial strain is difficult to determine as it is very dependent on the duration and rate of initial load and there is no clear distinction between initial strain and creep strain. Creep strain can be broken up into two parts, basic creep and drying creep. Basic creep is

“the increase in strain under sustained constant load of a concrete specimen in which moisture losses or gains are prevented.” Even after 30 years of measurement on sealed concrete specimens, it had yet to be determined if basic creep approaches an ultimate value. Drying creep is the additional creep occurring in a specimen exposed to the environment and allowed to dry. The effects of creep can be expressed in three ways. The first is similar to that of shrinkage, where creep strain is simply expressed in terms of microstrain (strain $\times 10^{-6}$). The second way is called the creep coefficient. The creep coefficient is the ratio of creep strain to the initial strain at loading. The third is specific creep. Specific creep is the ratio of microstrain to applied load (psi).

1.5.2. Factors Affecting Creep. Like shrinkage, creep is affected by numerous material, mix design, environmental, and construction related factors. Similar to shrinkage, the amount, size, gradation, and properties of the aggregate are very influential on creep of concrete. An increase in aggregate volume will decrease creep. Aggregate gradation is believed to influence creep of concrete because of its relation to changes in overall aggregate volume. The size of aggregate affects bond between paste and aggregate, which controls stress concentration and microcracking. Unlike shrinkage, which is primarily affected by properties of the paste, creep is very dependent on the elastic properties of the aggregate. Concretes with aggregate that have a lower modulus of elasticity generally have higher creep. The primary environmental factor in creep is relative humidity. As relative humidity increases, drying creep significantly decreases. Specimens in environments where drying cannot occur may have only one quarter of the creep of concrete which is allowed to dry. The effects of construction and design on creep are slightly different than shrinkage. One similarity is that increased curing time

will decrease creep strain. Unlike shrinkage, basic creep is not affected by the size and shape of the member. The factor that most affects creep is the load applied to the specimen. The magnitude of the load, and the age at which the load is first applied are very important. Loads up to $0.40f'_c$ are considered to be linearly related to creep. Finally, concrete loaded at later ages has lower creep.

1.6. CREEP MODELS

As with shrinkage, considerable research has been done and models developed to predict the creep potential of concrete. The following sections will present various models for calculating creep. This includes industry models developed for use with conventional concrete as well as models developed specifically for self-consolidating concrete.

1.6.1. ACI 209R-92. This model is based on the same research as the ACI 209 shrinkage model. The standard conditions as shown in **Table 1.1** apply to creep as well. **Eq. 1.50 – 1.52** represent the general model for concrete meeting the standard conditions. If standard conditions are met, γ_c is taken to be equal to 1. Like the shrinkage model, if any or all of the standard conditions are not met, the model modification factors must be used as shown in **Eq. 1.50 – 1.59**.

$$\Phi(t, t_0) = \frac{(t-t_0)^\psi}{d+(t-t_0)^\psi} \Phi_u \quad (1.50)$$

$$\Phi_u = 2.35\gamma_c \quad (1.51)$$

$$d = 26.0e^{\{0.36(V/S)\}} \quad (1.52)$$

$$\gamma_c = \gamma_{c,t_0} \gamma_{c,RH} \gamma_{c,vs} \gamma_{c,s} \gamma_{c,\psi} \gamma_{c,\alpha} \quad (1.53)$$

$$\gamma_{c,t_0} = \begin{cases} 1.25t_0^{-0.118} & \text{for moist curing} \\ 1.13t_0^{-0.094} & \text{for steam curing} \end{cases} \quad (1.54)$$

$$\gamma_{c,RH} = 1.27 - 0.67h \quad (1.55)$$

$$\gamma_{c,vs} = \frac{2}{3} (1 + 1.13e^{\{-0.54(V/S)\}}) \quad (1.56)$$

$$\gamma_{c,s} = 0.82 + 0.067s \quad (1.57)$$

$$\gamma_{c,\psi} = 0.88 + 0.0024\psi \quad (1.58)$$

$$\gamma_{c,\alpha} = 0.46 + 0.09\alpha \geq 1 \quad (1.59)$$

Where: $\Phi(t,t_0)$ is the calculated creep coefficient at a given age, Φ_u is the calculated ultimate creep coefficient, t is the age of the specimen in days, γ_{c,t_0} is the curing condition correction factor, t_0 is the age at which the specimen is loaded in days, $\gamma_{c,RH}$ is the humidity correction factor, h is relative humidity in decimals, $\gamma_{c,vs}$ is the size correction factor, V/S is the volume to surface area ratio, $\gamma_{c,s}$ is the slump correction factor, s is slump in inches, $\gamma_{c,\psi}$ is the fine aggregate correction factor, ψ is the ratio of fine aggregate to total aggregate by weight expressed as percentage, $\gamma_{c,\alpha}$ is the air content correction factor, and α is the air content in percent. For shape and size effects to be totally

considered, d is to be determined using **Eq. 1.52** and ψ assumed to be equal to 1.0. Otherwise, average values of $d=10$ and $\psi=0.6$ are to be assumed.

1.6.2. NCHRP Report 496. This proposed creep model was developed in a similar manner to that of the NCHRP Report 496 shrinkage model. The correction factors that are identical to those used in the corresponding shrinkage model have already been defined in Section 1.3.2. The model is shown in **Eq. 1.60 – 1.66**.

$$\psi(t, t_i) = 1.90\gamma_{cr} \quad (1.60)$$

$$\gamma_{cr} = k_{td}k_{la}k_s k_{hc}k_f \quad (1.61)$$

$$k_{td} = \frac{t}{61-4f'_{ci}+t} \quad (1.62)$$

$$k_{la} = t_i^{-0.118} \quad (1.63)$$

$$k_s = \frac{1064-94V/S}{735} \quad (1.64)$$

$$k_{hc} = 1.56 - 0.008H \quad (1.65)$$

$$k_f = \frac{5}{1+f'_{ci}} \quad (1.66)$$

Where: $\psi(t, t_i)$ is the calculated creep coefficient at a given age, k_{td} is the time development factor, t is the age of the concrete in days, k_{ta} is the loading factor, t_i is the age at which creep specimen is loaded in days, k_s is the size factor, V/S is the volume to surface area ratio, k_{hc} is the humidity factor, H is the average ambient relative humidity in percent, k_f is the concrete strength factor, and f'_{ci} is the specified compressive strength of concrete in ksi.

1.6.3. CEB-FIP 90. The following equations apply to the creep model as developed jointly by CEB and FIP as presented in the CEB-FIP Model Code 1990.

$$\Phi(t, t_0) = \Phi_0 \beta_c(t - t_0) \quad (1.67)$$

$$\Phi_0 = \Phi_{RH} \beta(f_{cm}) \beta(t_0) \quad (1.68)$$

$$\Phi_{RH} = 1 + \frac{1 - RH}{0.46 \left(\frac{2A_c}{100u} \right)^{1/3}} \quad (1.69)$$

$$\beta(f_{cm}) = \frac{5.3}{(f_{cm}/10)^{0.5}} \quad (1.70)$$

$$\beta(t_0) = \frac{1}{0.1 + t_0^{0.2}} \quad (1.71)$$

$$\beta_c(t - t_0) = \left[\frac{(t - t_0)}{\beta_H + (t - t_0)} \right]^{0.3} \quad (1.72)$$

$$\beta_H = 150 \{ 1 + (1.2RH)^{18} \} \left(\frac{2A_c}{100u} \right) + 250 \leq 1500 \quad (1.73)$$

Where: $\Phi(t, t_0)$ is the calculated creep coefficient at a given age, Φ_0 is the notional creep coefficient, β_c is the coefficient to describe the development of creep with time after loading, t is the age of concrete in days, t_0 is the age of concrete at loading in days, RH is the relative humidity in decimals, A_c is the cross section area in mm^2 , u is the perimeter in contact with the atmosphere in mm, and f_{cm} is the mean compressive strength of concrete at the age of 28 days in MPa.

1.6.4. GL 2000. As with the GL 2000 shrinkage model, the following creep model was published in the ACI materials journal under the title “Design Provisions for Drying Shrinkage and Creep of Normal-Strength Concrete”.

$$\Phi_{28} = \Phi(t_c) \left[2 \left(\frac{(t-t_c)^{0.3}}{(t-t_c)^{0.3}+14} \right) + \left(\frac{7}{t_0} \right)^{0.5} \left(\frac{t-t_c}{t-t_c+7} \right)^{0.5} + 2.5(1 - 1.086h^2) \left(\frac{t-t_0}{t-t_0+97(V/S)^2} \right)^{0.5} \right] \quad (1.74)$$

$$\Phi(t_c) = \left[1 - \left(\frac{t-t_c}{t-t_c+97(V/S)^2} \right)^{0.5} \right]^{0.5} \quad (1.75)$$

Where: Φ_{28} is the calculated creep coefficient at a given age, $\Phi(t_c)$ is a factor that takes into account drying before loading, t is age of concrete in days, t_c is the age of concrete when drying begins, t_0 is the age the concrete was loaded, h is humidity in decimals, and V/S is the volume to surface area ratio in mm.

1.7. SCC CREEP RESEARCH

1.7.1. NCHRP Report 628. As with shrinkage, NCHRP 628 presents an SCC specific creep prediction model which is a modified version of the AASHTO 2004 model. **Eq. 1.76 – 1.81** are used to calculate creep of SCC using the proposed modification factor.

$$\psi(t, t_i) = 1.9k_{vs}k_{hc}k_fk_{td}k_i^{-0.118} \times A \quad (1.76)$$

$$k_{vs} = 1.45 - 0.0051(V/S) \geq 0 \quad (1.77)$$

$$k_{hc} = 1.56 - 0.08H \quad (1.78)$$

$$k_f = \frac{35}{7+f'_{ci}} \quad (1.79)$$

$$k_{td} = \left(\frac{t}{61 - 0.58f'_{ci} + t} \right) \quad (1.80)$$

$$A = \begin{cases} 1.19 & \text{for Type I/II cement} \\ 1.35 & \text{for Type III cement} \end{cases} \quad (1.81)$$

Where: $\psi(t, t_i)$ is the calculated creep coefficient, k_{vs} is the volume to surface area factor, V/S is the volume to surface area ratio, k_{hc} is the humidity correction factor, H is relative humidity in percent, k_f is the concrete strength factor, f'_{ci} is the concrete compressive strength at time of loading in MPa, k_{td} is the time development factor, t is age of concrete since loading in days, and A is the cement type correction factor.

1.7.2. Long and Khayat. A total of 16 SCC mixes were tested for creep. The purpose of this experimental program was to determine the key mixture design and material selection parameters that most affect creep of SCC. Additionally, conclusions were made on which current creep prediction model best estimates creep of SCC. It was found that the binder type (i.e. cementitious materials) was most influential on creep of SCC, followed by binder content. The model that best predicts creep of SCC was found to be CEB-FIP 90. The modified AASHTO model described in Section 1.7.1. was also determined to successfully predict creep of SCC.

1.7.3. Long, et. al. The same study as described in Section 1.4.4 was also done to develop a prediction equation for creep strain of SCC. The following equation was developed to predict creep of SCC, with the same variable definitions as shown in **Table 1.2.**

112 day creep strain ($\mu\epsilon$):

$$\begin{aligned} &+1036 + 73.6 BT + 40.7 (VMA \cdot BT) + 38.8 BC \\ &+34.9 (w/cm \cdot BT) - 32.9 (BC \cdot S/A) \end{aligned} \quad (1.82)$$

1.8. Application of Shrinkage and Creep

1.8.1. Prestress Loss. Prestress loss is “the loss of compressive force acting on the concrete component of a prestressed concrete section.” (NCHRP 426) The ability to accurately predict the prestress loss in beams is very dependent on the ability to predict the beam’s shortening due to shrinkage and creep. Shortening of the beam reduces the tensile force in the prestressed reinforcement and must be accounted for in design.

NCHRP 426 names three components which significantly affect the prestress loss in pretensioned concrete members which directly relate to shrinkage and creep. These components are:

1. Instantaneous prestress loss due to elastic shortening at transfer of force from prestressed reinforcement to concrete.
2. Long-term prestress loss due to shrinkage and creep of concrete and relaxation of prestressing strands between the time of transfer and deck placement.
3. Long-term prestress loss between the time of deck placement to the final service life of the structure due to shrinkage and creep of the girder.

Figure 1.2 shows the prestress loss over the life cycle of a pretensioned concrete girder. The loss between points D and E represent the loss due to creep, shrinkage, and relaxation of prestressing strands.

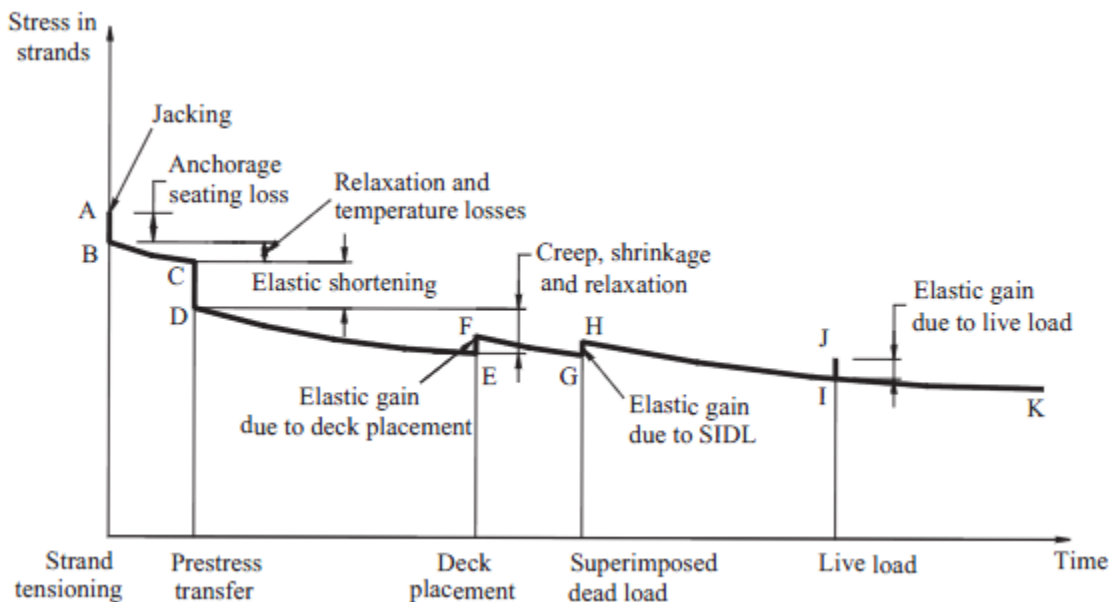


Figure 1.2 - Stress vs. Time for Prestressed Bridge Girder (Tadros et. al. 2003)

1.8.2. Load Effects. The procedures in “Design of Continuous Highway Bridges with Precast, Prestressed Concrete Girders” published by the Portland Cement Association (PCA) take into account additional moments due to shrinkage and creep when determining loads for design. In this method, fixed end moments due to creep and end driving moments due to shrinkage are calculated. These applied moments result from a continuity connection being made at supports by the placement of the bridge deck. The placement restricts free rotation of the beams and therefore produces moment in the connection. The moments calculated by this method are then added to all other load effects at all sections for determination of the ultimate design load. The shrinkage driving moment calculation is done by first calculating theoretical ultimate shrinkage values for the beam and the slab. The differential shrinkage between the beam and slab are then used to determine an applied moment due to shrinkage. The applied moment due to creep results from prestressed creep and dead load creep. Theoretical creep coefficients are calculated for the time before and after deck placement. The creep that occurs after deck placement is what contributes to the applied moment.

1.8.3. Beam Deflection. Shrinkage and creep must also be accounted for when calculating long term deflection of flexural members. Eq. 9-11 of ACI 318-08, shown here as **Eq. 1.83**, accounts for long term sustained loads. This factor is multiplied by the immediate deflection caused by the load considered.

$$\lambda_{\Delta} = \frac{\xi}{1+50\rho'} \quad (1.83)$$

Where: λ_{Δ} is the multiplier for additional deflection due to long-term effects, ξ is the time dependent factor for sustained load, and ρ' is compression reinforcement ratio.

1.9. CONCRETE ABRASION

1.9.1. Definition of Concrete Abrasion. Abrasion is the physical wearing down of a material. The most common sources of abrasion of concrete structures are by the friction between vehicle tires and concrete pavement road surfaces, and by water flows over exposed dam or bridge footings. Concrete abrasion leads to a decrease in member thickness which can lead to cracking or failure of the structure (Atis).

1.9.2. Factors Affecting Concrete Abrasion. Several material properties and construction factors can affect the abrasion resistance of concrete. The concrete strength is the most influential property in regards to abrasion resistance. The properties of the aggregate are also very important in a concrete's resistance to abrasion. The surface finish and whether or not a hardener or topping is used effects abrasion resistance as well (Naik et. al.).

1.10. SCC ABRASION RESEARCH

Little research has been done on self-consolidating concrete's abrasion resistance relative to conventional concrete. This is most likely due to the fact that the use of SCC is not motivated primarily by its hardened properties but by its fresh concrete properties. Also SCC members are less likely to be exposed to abrasive action as SCC is normally reserved for use in pre-stressed members such as girders which are typically not exposed to vehicles or water.

2. RESEARCH PROGRAM

2.1. MIX DESIGNS

2.1.1. SCC. The SCC testing program consisted of four mixes, two being SCC with two as conventional concrete equivalents to the SCC mixes. The naming convention used in the SCC testing program begins with either C (conventional concrete) or S (SCC). The next number indicates the target 28 day compressive strength, in ksi. Following the dash is a number indicating the ratio of fine aggregate to total aggregate by weight. It finishes with L, indicating the type of coarse aggregate used, dolomitic limestone. The baseline normal strength concrete tested was MoDOT A-1 (C6-58L). The A-1 mix was used as the comparative mix to the normal strength SCC mix (S6-48L). Both mixes had identical w/c and air content, with the aggregate ratio and HRWR dosage adjusted. The S6-28L mix design was based on the average of survey responses from regional precast plants. The baseline high strength concrete (C10-58L) mix design was based on research done by Myers and Carrasquillo (2000) at the University of Texas at Austin. The high strength SCC mix (S10-48L) was designed based on the C10-58L mix design and finalized after trial batches were made and adjusted. The designs of the mixes tested can be found in **Table 2.1** along with measured 28 day compressive strength (f'_c) and modulus of elasticity (MOE). All mixes and specimens were batched and cast in the Missouri University of Science and Technology (Missouri S&T) concrete lab located in Butler-Carlton Hall. All testing was done in the High Bay Structures Engineering Laboratory (SERL) also located in Butler-Carlton Hall on the campus of Missouri S&T. Due to the large volume of concrete produced for various studies associated with this overall research program (i.e. Reports A, B, C, D, and E) some concrete production was

done in separate batches on different days resulting in some minor variations in concrete properties between various reports.

Table 2.1 - SCC Test Program Mix Designs and mechanical properties

Material	Amount (per cubic yard)			
	C6-58L	S6-48L	C10-58L	S10-48L
Water	277.5 lb.	277.5 lb.	315 lb.	315 lb.
Cement	750 lb. (Type I)	750 lb. (Type I)	840 lb. (Type III)	840 lb. (Type III)
Coarse Aggregate	1610 lb.	1333 lb.	1440 lb.	1192 lb.
Fine Aggregate	1444 lb.	1444 lb.	1043 lb.	1291 lb.
Fly Ash	N/A	N/A	210 lb.	210 lb.
BASF MB-AE-90 (air entrainment)	2.3 fl oz/cwt	1.2 fl oz/cwt	1.25 fl oz/cwt	1.0 fl oz/cwt
BASF Glenium (HRWR)	4.7 fl oz/cwt	6.2 fl oz/cwt	4.9 fl oz/cwt	6.0 fl oz/cwt
f'c (psi)	7,000	5,500	11,000	13,500
MOE (psi)	3,450,000	3,130,000	3,900,000	4,200,000

Conversion: $1 \text{ kg/m}^3 = 1.686 \text{ lb/yd}^3$

1 fl oz = 26.57 mL

1 psi = 6.89 kPa

2.2. SHRINKAGE AND CREEP SPECIMEN CONSTRUCTION

2.2.1. Shrinkage and Creep Specimens. Both shrinkage and creep testing were done using identical specimens. Although only four specimens per mix were necessary for testing (two each for shrinkage and creep), six specimens per mix were cast in case any specimens were damaged during de-molding. These specimens were fabricated and prepared as described below.

2.2.2. Shrinkage and Creep Molds. The molds for the shrinkage and creep specimens were 4 in. diameter PVC pipe adhered to a plywood base. The PVC was cut into 24 in. sections with care being taken to ensure all cuts were made so that the mold would sit flush and orthogonal to the base. The PVC was also notched on opposite sides. The notches made de-molding much easier and significantly reduced the possibility of damaging the specimens during de-molding. Once prepared the PVC was adhered to a 1 ft. (304.8 mm) by 1 ft. (304.8 mm) plywood base using a waterproof silicon sealant. The completed molds were allowed to sit for at least 24 hours before use to allow for the sealant to fully set up. **Figure 2.1** shows a completed shrinkage and creep mold.



Figure 2.1 - Shrinkage and Creep Form

2.2.3. Shrinkage and Creep Specimen Casting. Specimens were consolidated in a manner similar to that prescribed in ASTM C31 “Standard Practice for Making and Curing Concrete Test Specimens in the Field” for a 6 in. diameter cylinder.

Consolidation and vibration were performed when necessary. The specimens were cast in three layers of approximately equal depth and were rodded 25 times per layer for all mixes. External vibration was also performed after each layer was rodded using an electric handheld concrete vibrator as needed. Specimens were moist cured until de-molded and prepared.

2.2.4. Shrinkage and Creep De-Molding and Preparation. All specimens were de-molded within 24 hours of their initial set time. De-molding was done by first cutting through the notched section with a utility knife. A hammer and chisel were then used to split the mold and remove it from the concrete. Creep specimens were sulfur capped on both ends in preparation for loading at 28 days. Shrinkage specimens were sulfur capped on only the bottom end, allowing for stability and more accurate readings.

2.2.5. Shrinkage and Creep Data Acquisition. A demountable mechanical strain gauge (DEMEC) was used to measure strain in the concrete. DEMEC points, small pre-drilled stainless steel discs, were adhered to the surface of the specimen. They were arranged in three vertical lines of five points, 120° apart, as shown in **Fig. 2.2**. This arrangement allowed for 9 readings to be taken per specimen. The average of all readings taken per specimen was taken as the value to be used for strain calculation. The points in one line per specimen were adhered using gel control super glue. The instant hardening allowed for initial readings to be made on each specimen as soon as possible.

The remaining points were adhered using concrete/metal epoxy, which took up to 24 hours to fully harden for accurate reading to be taken. The points adhered with super glue were later protected using the epoxy.

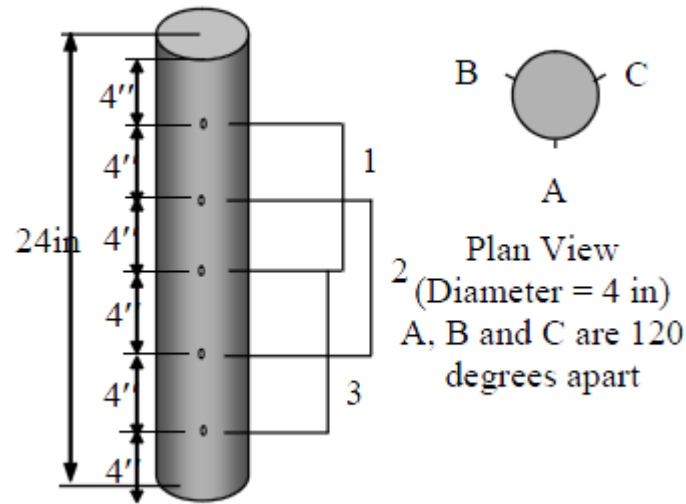


Figure 2.2 – Shrinkage and Creep Specimens and DEMEC Point Arrangement (Myers and Yang, 2005)

2.3. ABRASION SPECIMEN CONSTRUCTION

One specimen per mix was cast for abrasion test. Each specimen was large enough so that three replicate abrasion tests could be done for each mix. Abrasion specimens measured 6 in. (152.4 mm) by 16 in. (406.4 mm) by 3.5 in. (88.9 mm) and were cast in a mold made from wooden 2x4 sections and attached to a plywood base. The baseline mixes were consolidated similar to that prescribed in ASTM C31 “Standard Practice for Making and Curing Concrete Test Specimens in the Field” for a 6 in. (152.4 mm) wide beam. External vibration was used as necessary. To ensure that abrasion tests on all specimens were consistent, every specimen tested was finished by the same individual using a hand trowel. Specimens were moist cured until tested. All testing was performed on the top finished surface of the specimen.

2.4. TESTING PROCEDURES

2.4.1. Shrinkage Testing Procedures. A modified version of ASTM C157 “Standard Test Method for Length Change of Hardened Hydraulic-Cement Mortar and Concrete” was used to determine the shrinkage of the concrete specimens. Until the age of loading for creep, four specimens were used for shrinkage determination. At 28 days, two of these specimens were transferred to creep frames, leaving two remaining specimens to be tested for long term shrinkage. Nine strain readings could be taken per specimen, with the average of all readings taken as the value to be used for shrinkage calculation. Strain was determined using the DEMEC readings and calculated by **Eq. 2.1** as found in “Simplified Instructions for Using a Digital DEMEC Gauge”. An example of a DEMEC reading being taken on a specimen is shown in **Figure 2.3**. Readings were normalized by taking a reading on the reference bar (see **Figure 2.4**) as shown in **Figure 2.5**. Shrinkage strain experienced during the first day after demolding was estimated based on linear interpolation of subsequent strain values, as calculated by **Eq. 2.1**

$$\Delta\varepsilon_s = G((R_i - R_0) - (D_i - D_0)) \quad (\mu\varepsilon) \quad (2.1)$$

Where: $\Delta\varepsilon_s$ is the change in strain from one reading to the next, G is the gauge factor shown in **Figure 2.6**, 0.400×10^{-5} strain per division (4 microstrain), D_0 is the datum reading on the reference bar, D_i is the subsequent reading on the reference bar, R_0 is the datum reading on the tested material, and R_i is the subsequent reading on the tested material. Gauge units are the digital gauge reading without the decimal point. For example, **Figure 2.7** shows a reading of 2.523 which equates to 2523 gauge units.



Figure 2.3 – DEMEC Reading Taken on Specimen



Figure 2.4 - Reference Bar



Figure 2.5 - Reading Taken on Reference Bar



Figure 2.6 - Gauge Factor Used for Shrinkage and Creep Calculations



Figure 2.7 - Example DEMEC Gauge Reading

2.4.2. Creep Testing Procedures. A modified version of ASTM C512 “Standard Test Method for Creep of Concrete in Compression” was used to determine the creep of the concrete specimens tested. Until the age of loading, creep specimens acted as shrinkage specimens. This is a modification of ASTM C512, as the specimens were not moist cured beyond the time of de-molding. Additionally, humidity was not controlled however it was recorded.

At 28 days, representative specimens were tested according to ASTM C39 “Standard Test Method for Compressive Strength of Cylindrical Concrete Specimens” and ASTM C469 “Standard Test Method for Static Modulus of Elasticity and Poisson’s Ratio of Concrete in Compression.” Creep specimens were then loaded to 40% of their measured 28 day compressive strength in the creep frames shown in **Figures 2.8 – 2.9**. The design of the creep frames was based on research done by Myers and Yang (2005).

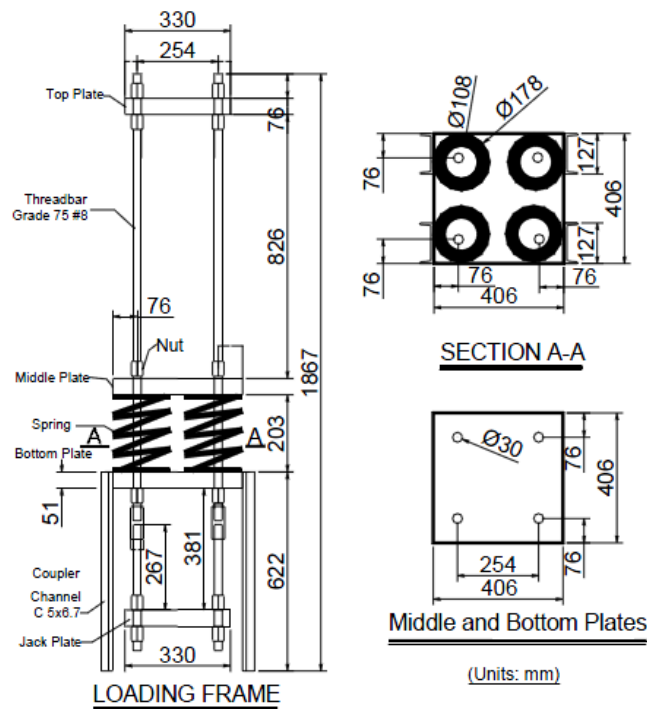


Figure 2.8 - Schematic of Creep Loading Frame (Myers and Yang, 2004)
(1 in = 25.4 mm)



Figure 2.9 - Creep Loading Frame with Specimen

Measurements taken on creep specimens were done in the exact way as with the shrinkage specimens. **Eq. 2.2** was used to determine the change in strain between one creep reading to the next. Using the calculated creep strain, the coefficient of creep could be determined by **Eq. 2.3**. Creep and shrinkage readings for like specimens were taken at the same interval. Readings were also taken immediately before and after loading to determine initial elastic strain due to loading. **Figure 2.10** shows a reading being taken on a creep specimen.

$$\Delta\varepsilon_c = G((R_i - R_0) - (D_i - D_0)) - \Delta\varepsilon_s \quad (\mu\varepsilon) \quad (2.2)$$

Where: $\Delta\varepsilon_c$ is the change in creep strain between readings.

$$\Phi(t, t_0) = \varepsilon_t / \varepsilon_i \quad (2.3)$$

Where: $\Phi(t, t_0)$ is the measured creep coefficient at a given age, ε_i is the measured strain due to initial loading of the specimen, ε_t is the measured creep strain at a given age.



Figure 2.10 - Reading Taken on Creep Specimen

2.4.3. Abrasion Resistance Testing Procedures. ASTM C944 “Standard Test Method for Abrasion Resistance of Concrete or Mortar Surfaces by the Rotating-Cutter Method” was used to determine abrasion resistance. A schematic of the rotating cutter used is shown in **Figure 2.11**, which is taken from ASTM C944. The actual rotating cutter is shown in **Figure 2.12**. Abrasion specimens were moist cured until testing at 28 days age. One specimen per mix was constructed, which allowed for three abrasion tests. One abrasion test consisted of three abrasion cycles. Each cycle lasted two minutes. A load of 44lb, defined as a double load in ASTM C944, was applied at a rate of 300 rpm using a drill press as shown in **Figure 2.13**. After each cycle, mass loss (mg) was recorded by subtracting the final weight from the initial weight. Each cycle per test was done on the same spot. After completion of each abrasion test, the average depth of wear (mm) was measured using digital calipers. The average depth of wear was calculated from a total of eight depth measurements relative to the adjacent untested surface, four taken on the outer perimeter of the tested surface and four taken around the inner perimeter, at the points indicated in **Figure 2.14**. The measurements were made using a digital caliper. On the day of testing, the specimen was removed from moist cure and surface dried by blotting with paper towels. This was done to avoid any mass loss due to moisture loss. A completed specimen after all three abrasion tests is shown in **Figure 2.15**.

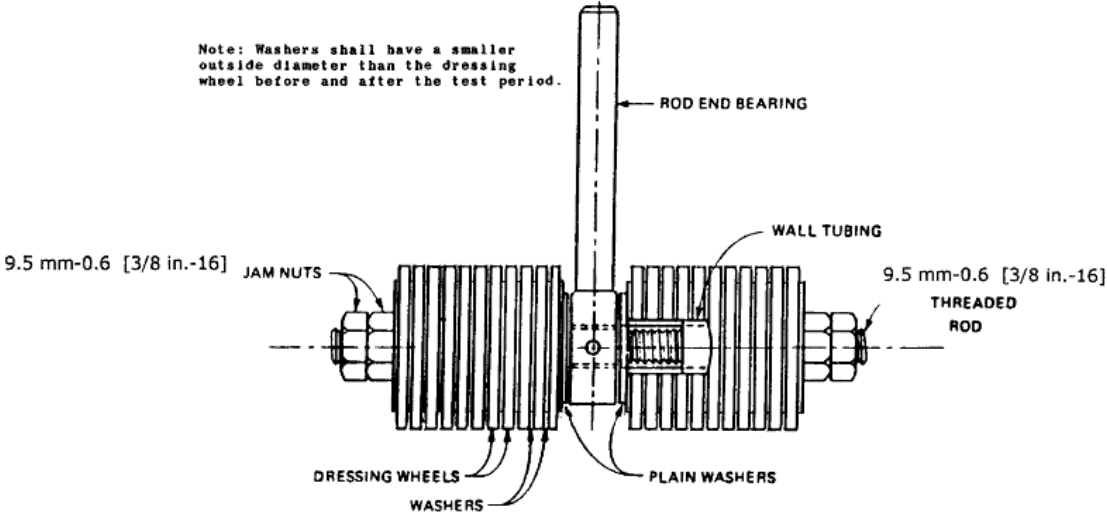


Figure 2.11 - Schematic of Abrasion Rotating Cutter (ASTM C944)
(1 in = 25.4 mm)



Figure 2.12 - Rotating Cutter



Figure 2.13 - Abrasion Resistance Test In Progress

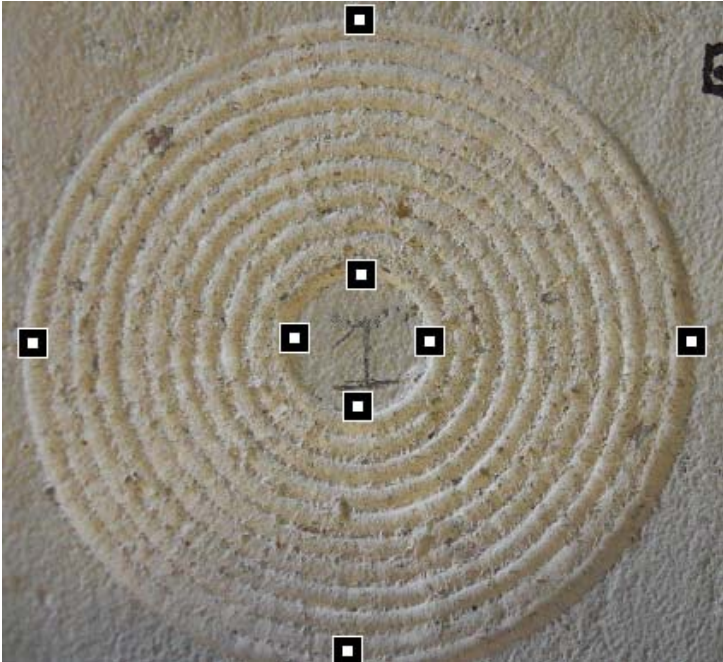


Figure 2.14 - Depth of Wear Measurement Points



Figure 2.15 - Abrasion Resistance Specimen After Testing

3. SCC RESULTS AND DISCUSSION

3.1. SHRINKAGE

3.1.1. Results. Figures 3.1 – 3.4 show the experimental data obtained from shrinkage tests of SCC plotted with the various prediction models discussed in Section 1. Figure 3.5 shows the experimental results of all four mixes plotted with one another. In figures where different data sources are together, the source of the data can be found in parentheses after the data label in the legend of its respective figure. All data obtained in this study was gathered at Missouri S&T.

3.1.2. Discussion and Conclusions. For the lower strength variations, C6-58L and S6-48L, the relative shrinkage strains are not consistent with the SCC prediction model found in NCHRP Report 628. This model was a modification of the AASHTO prediction model, with an added factor to account for the effects of SCC. In the NCHRP Report 628 model, SCC made using Type I/II cement should show a reduction in shrinkage strain. The reduction factor in NCHRP Report 628 for SCC with Type I/II cement is 0.918, therefore it is expected that S6-48L would have a reduction in shrinkage strain. The reason for this inconsistency with previous data could be the difference in mix designs used in this project compared to others. Since shrinkage of concrete is most related to shrinkage of paste, it would be expected that mixes with higher paste volumes would experience more shrinkage. Relative to all mixes tested by Schindler, et. al., S6-48L had a greater cement content, fine aggregate content, and FA/CA ratio. In a similar study done by Long, Khayat and Xing, it was concluded that shrinkage is highly affected by binder content. The relatively high binder content and low coarse aggregate content of S6-48L could be the reason for the large shrinkage strains.

For high strength variations, C10-58L and S10-48L, the experimental results are very consistent with previous findings. Schindler, et. al. reported that high strength SCC mixes show a reduction in shrinkage relative to high strength conventional concrete. Therefore it can be expected that, in terms of shrinkage, high strength SCC is an adequate alternative to conventional high strength concrete.

Besides the mix designs themselves, the environment the specimens were exposed to seemed to have a significant effect on shrinkage. As seen in Appendix A, there is a correlation between shrinkage and relative humidity. The unexpected decreases in shrinkage that were measured tend to correspond to days with unusually high relative humidity. This confirms the relationship given by **Eq. 1.1** from ACI 209.1R-05 which states that shrinkage is inversely related to relative humidity.

Comparing the results to previous studies, both SCC mixes perform adequately. **Table 3.1** and **Figure 3.6** show the shrinkage data of S6-48L and S10-48L relative to the database compiled in Fernandez-Gomez and Landsberger, Shindler et. al., and Holshemacher and the equations developed by Long, et.al. The 112 day shrinkage strains calculated from Long et. al. are the 56 day autogenous shrinkage (**Eq. 1.48**) added to the 112 day drying shrinkage (**Eq. 1.49**). This is acceptable as it has been shown that autogenous shrinkage reaches stable values after 56 days (Long, Khayat, and Xing). Results from this study are consistent with the database compiled by Fernandez-Gomez and Landsberger, which includes 93 SCC mixes. At all ages that were tested in this study the results for both S6-48L and S10-48L fall within the limits of the database. When comparing to the shrinkage prediction equations developed by Long et. al., however, S6-48L doesn't seem to perform quite as well. Again, when comparing S10-48L to this

previous SCC shrinkage study, it performs very well. Below is a summary figure showing the SCC mixes tested in this program shown with the databases compiled by Fernandez-Gomez and Landsberger, Shindler et. al., and Holschemacher. The shrinkage from Schindler et. al. is likely lower due to the specimens being submerged in a lime bath for the first 7 days.

Finally, results for the normal strength variations are consistent with the observation made by Holschemacher (2004) that “In the majority of the evaluated data the shrinkage of SCC is 10 to 50% higher than the one of conventional concrete.” At 150 days, S6-48L had experienced 24% greater shrinkage than C10-58L. This trend, however, does not hold true for the high strength variations.

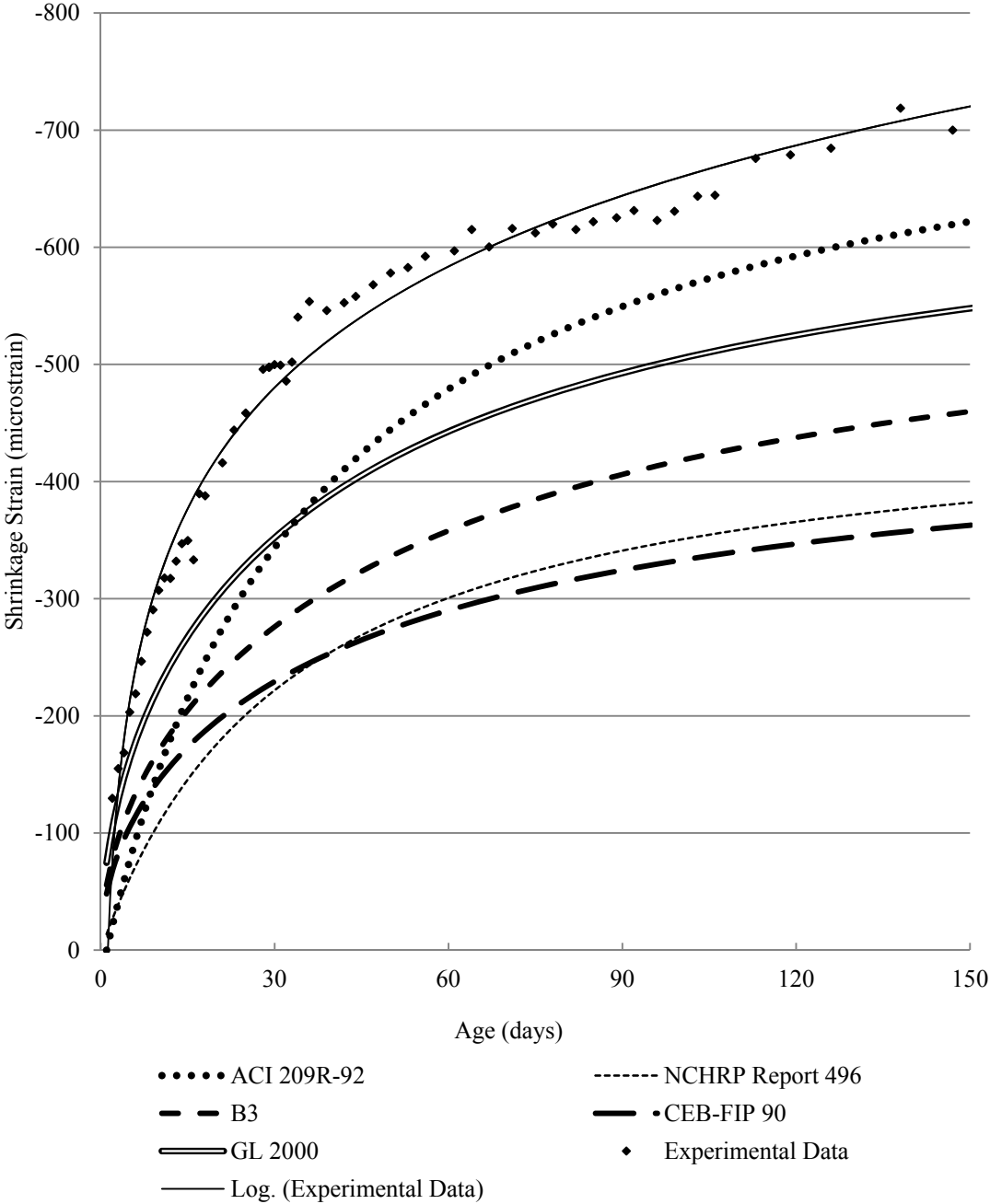


Figure 3.1 - C6-58L Shrinkage Results and Prediction Models

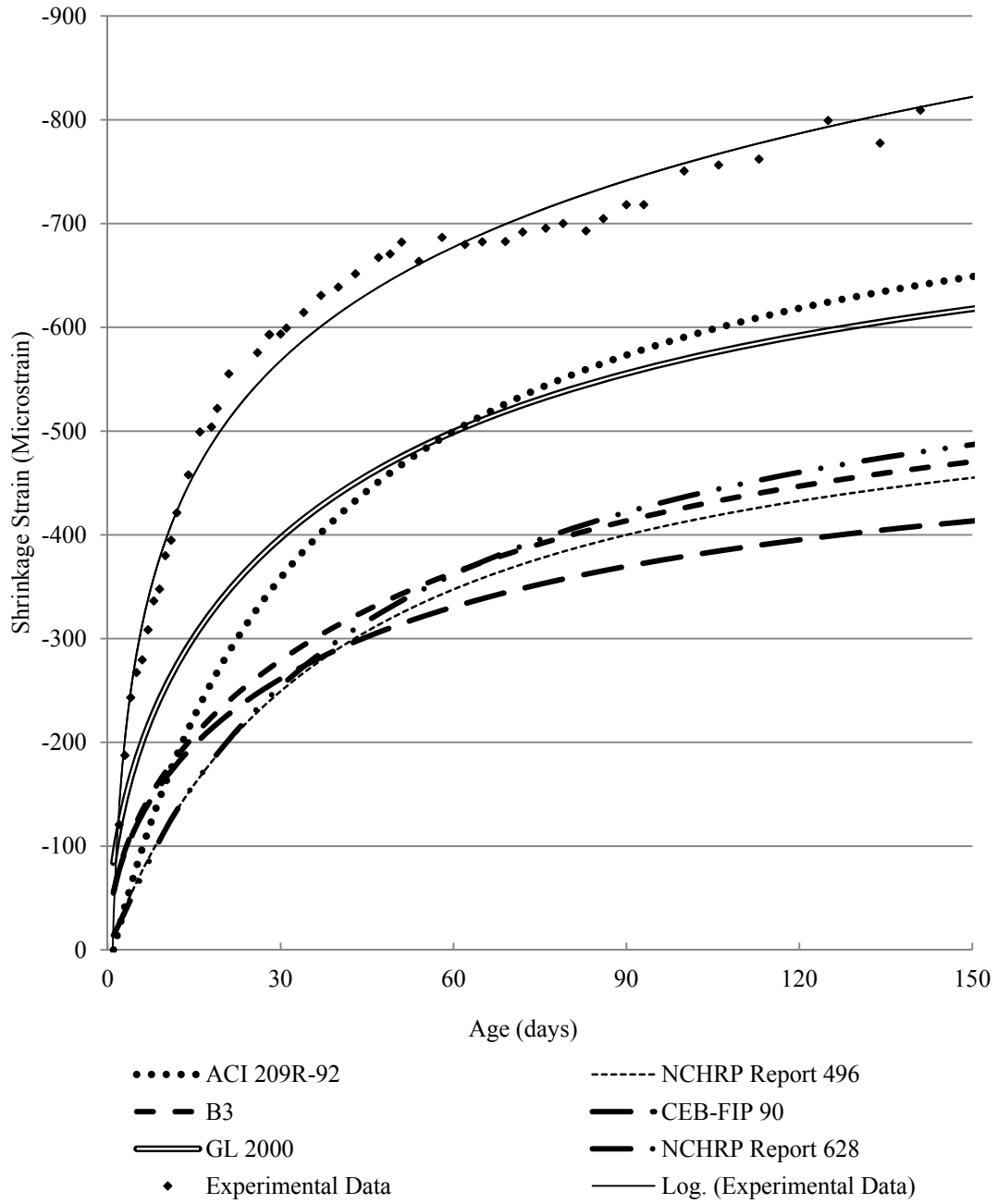


Figure 3.2 - S6-48L Shrinkage Results and Prediction Models

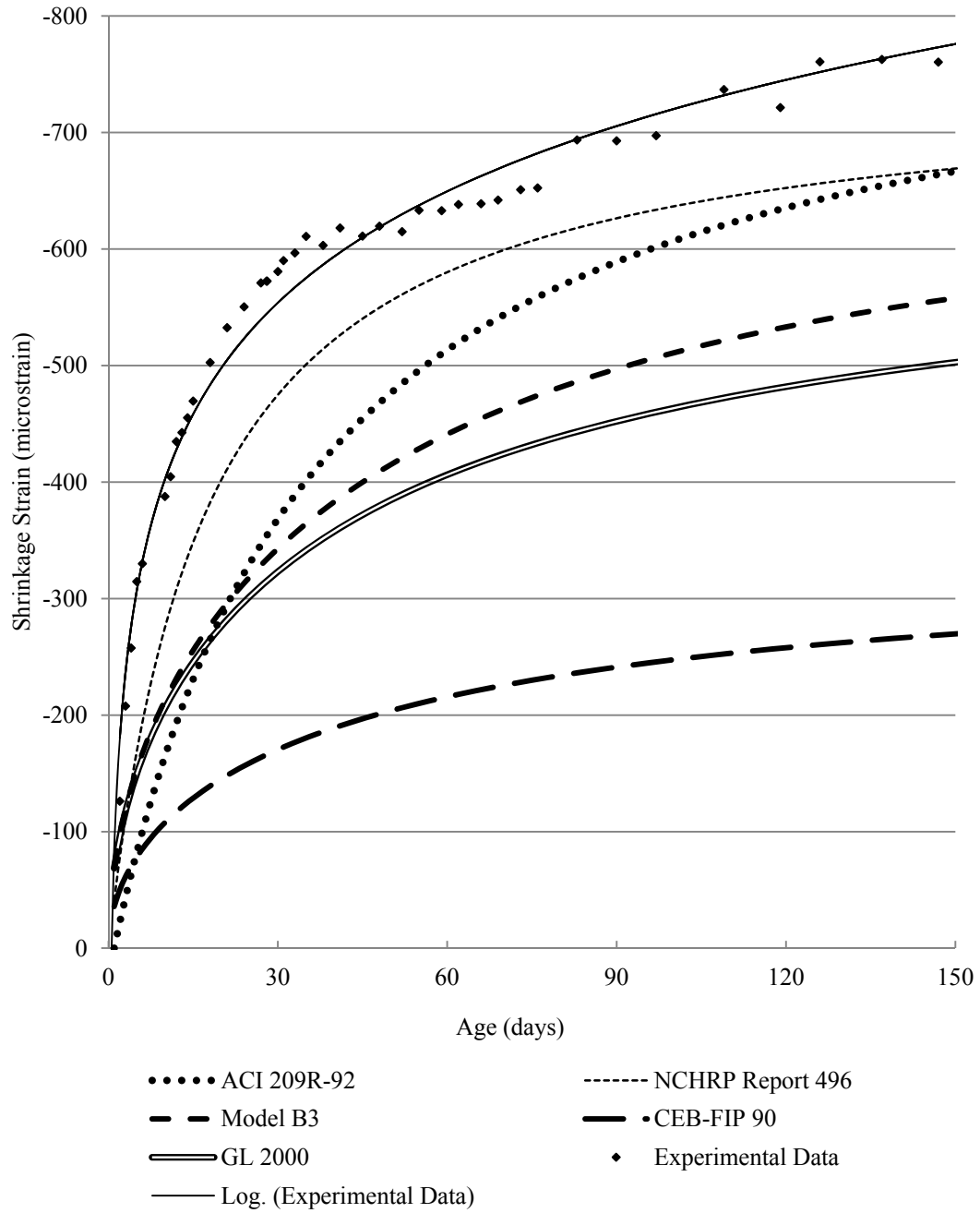


Figure 3.3 - C10-58L Shrinkage Results and Prediction Models

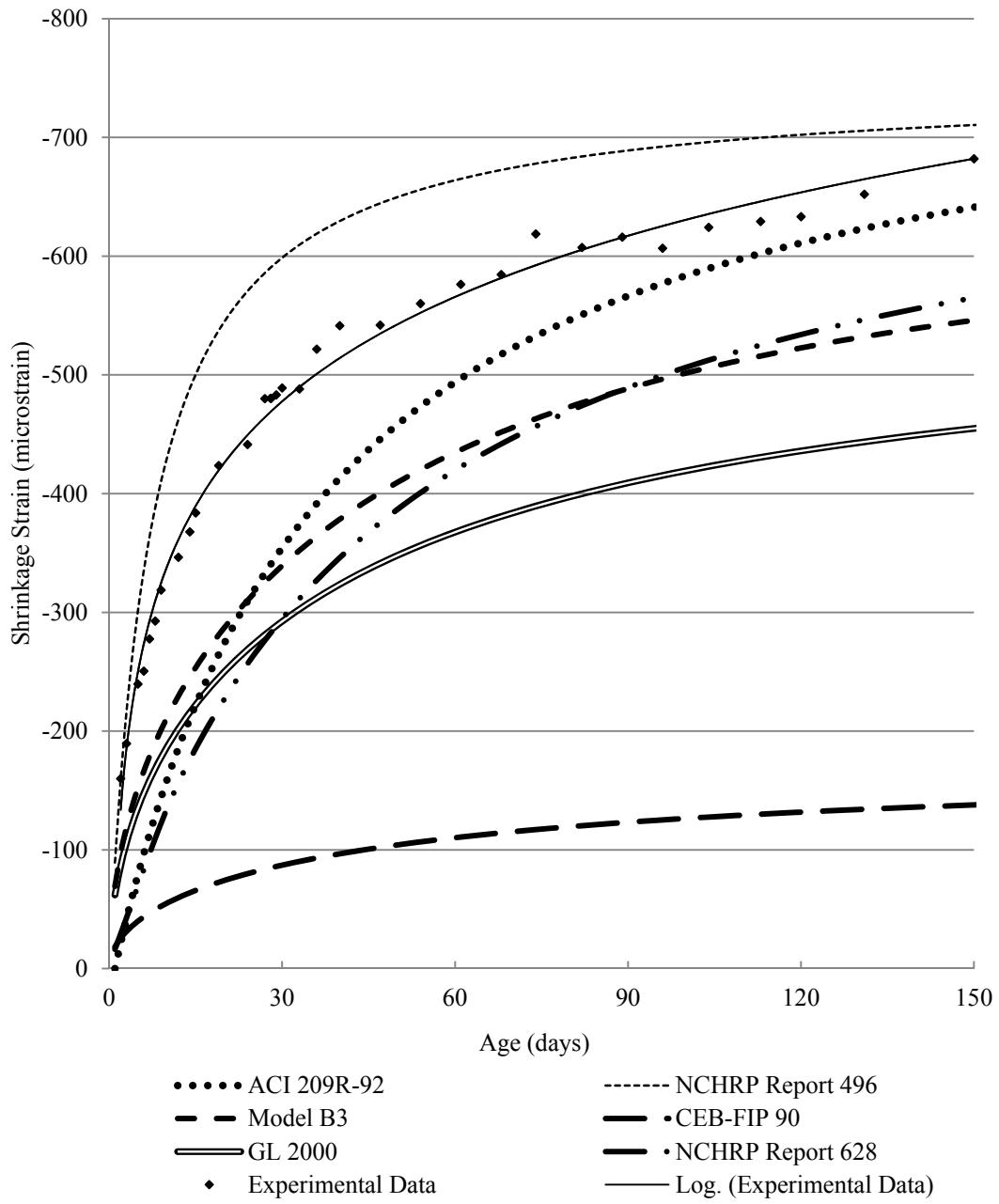


Figure 3.4 - S10-58L Shrinkage Results and Prediction Models

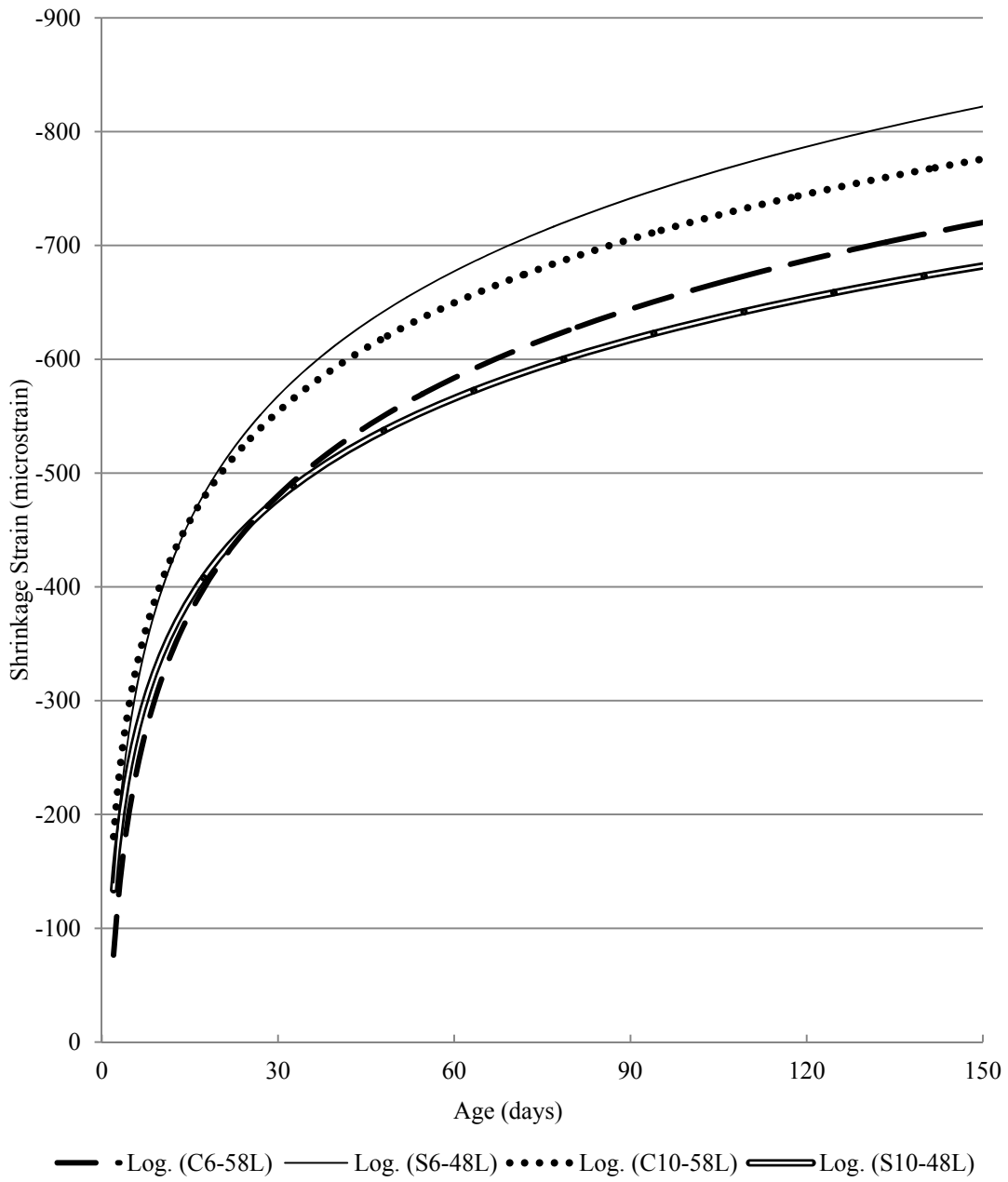


Figure 3.5 - SCC Shrinkage Results (Best fit Logarithmic)

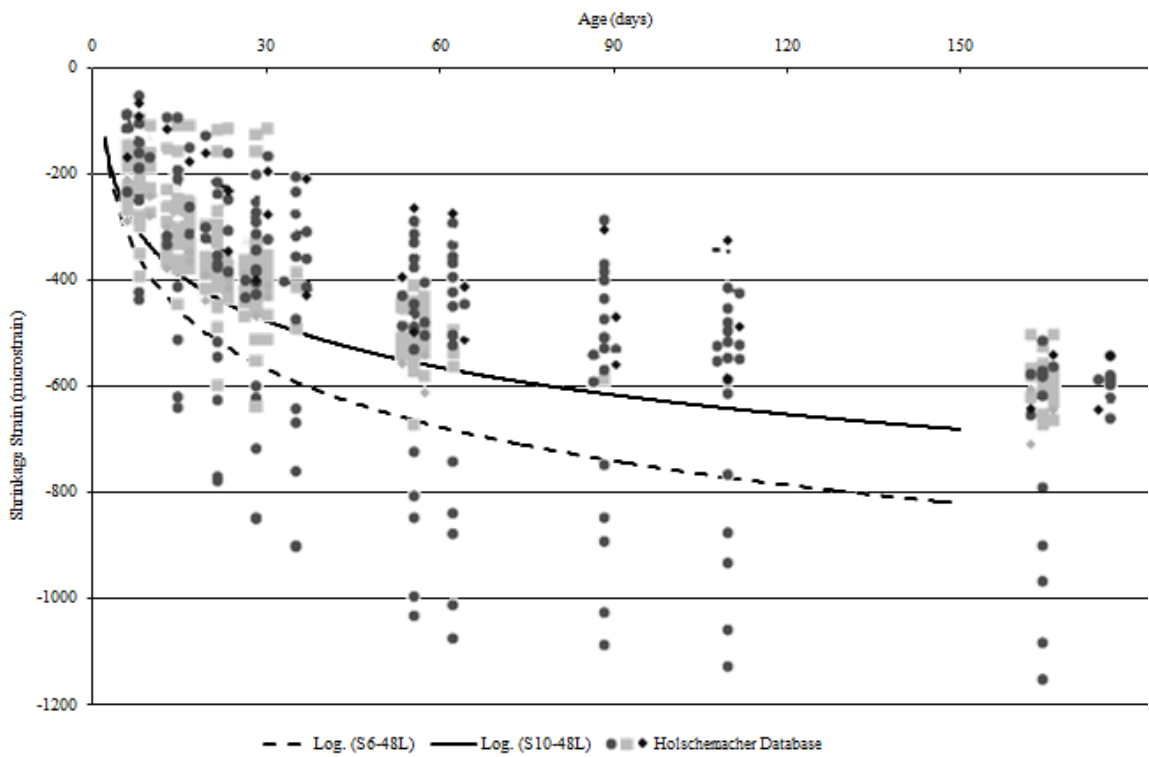
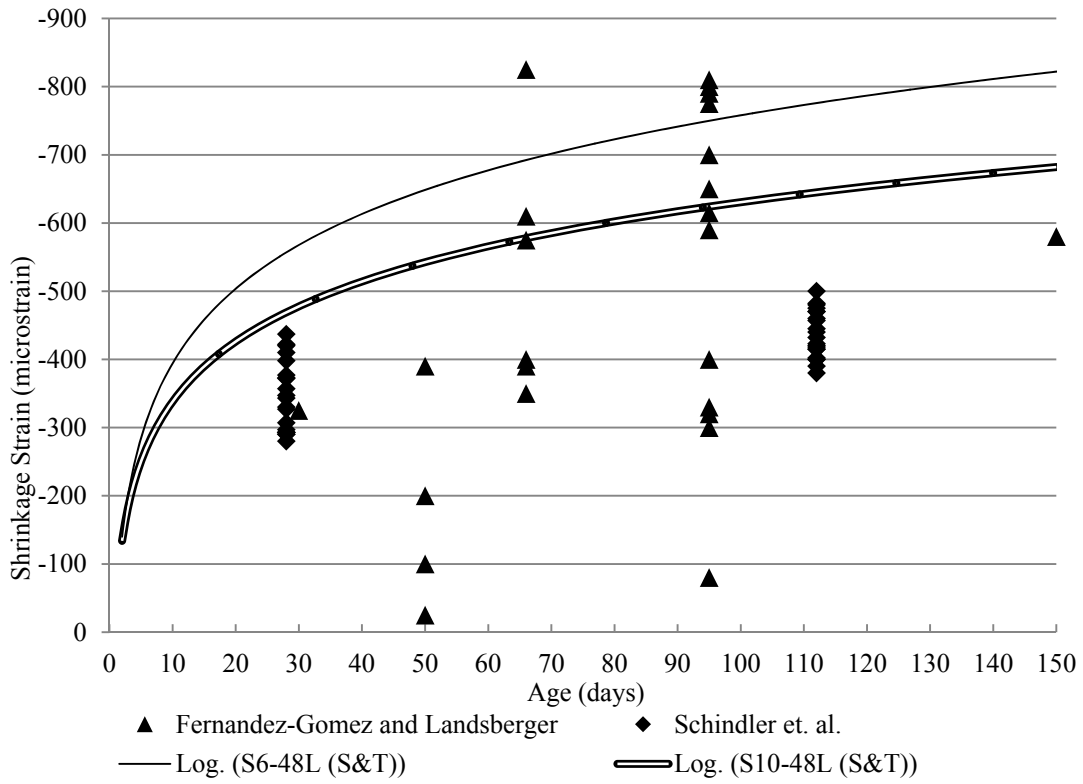


Figure 3.6 – SCC Results with Shrinkage Databases (Fernandez-Gomez, Shindler et. al., and Holschemacher)

Table 3.1 – SCC results compared to Eqs. 2.48 – 2.49 by Long et. al.

Specimen	112 Day Measured Shrinkage Strain (microstrain)	112 Day Theoretical Shrinkage Strain (microstrain)
S6-48L	-761	-659
S10-48L	-628	-1029

3.2. CREEP

3.2.1. Results. Creep Results are shown in **Table 3.2** and **Figure 3.7**. In figures where different data sources are together, the source of the data can be found in parentheses after the data label in the legend of its respective figure. For all specimens tested for this study, the notation (S&T) will be used.

Table 3.2 - Summary of SCC Creep Results

Creep Strain (microstrain)				
Specimen	Days After Loading			
	7	14	56	126
C6-58L	282	329	608	862
S6-48L	196	272	592	928
C10-58L	371	452	949	1326
S10-48L	441	557	874	1005
Percentage of 126 Day Creep				
C6-58L	33	38	71	100
S6-48L	21	29	64	100
C10-58L	28	34	72	100
S10-48L	44	55	87	100
Measured Creep Coefficient				
C6-58L	0.387	0.451	0.834	1.18
S6-48L	0.477	0.660	1.44	2.25
C10-58L	0.423	0.516	1.08	1.51
S10-48L	0.388	0.489	0.768	0.883
Specific Creep ($\mu\epsilon/\text{psi}$)				
C6-58L	0.101	0.118	0.217	0.308
S6-48L	0.089	0.124	0.269	0.422
C10-58L	0.085	0.103	0.216	0.302
S10-48L	0.082	0.104	0.163	0.188

Conversion: 1 MPa = 145.04 psi

3.2.2. Discussion and Conclusions. Like the shrinkage results, for normal strength specimens, the conventional concrete variation outperformed SCC. Also like the shrinkage results, for the high strength specimens, SCC outperformed conventional concrete.

For normal strength concrete, these results are supported by every prediction model that was analyzed. Every model predicts that C6-58L would have a lower creep coefficient than S6-48L after 126 days being loaded. The models were not as consistent when predicting the creep behavior of high strength concrete. The model identified by Long and Khayat (2011) as best predicting SCC creep behavior, CEB-FIP 90, does predict the behavior of specimens in this study. CEB-FIP 90 predicts that, like the results, S10-48L would have a lower creep coefficient than C10-58L after 126 days being loaded. Additionally, NCHRP Report 628 (2009), the model which is specifically for SCC, also predicts the same relationship.

In terms of comparing the results to previous research, both specimens performed very well. Long and Khayat (2011) investigated the creep strain on 16 SCC mixes. Eight of these mixes Nos. 1-8, were all very similar to S6-48L in terms of compressive strength, with Nos. 1-4 having a w/c of .34 and Nos. 5-8 with a w/c of .40. When plotted against these mixes, as shown in **Figure 3.8**, S6-48L performs very well. The same relationship exists between S10-48L and Nos. 9-12 from Long and Khayat (2011). These mixes have a similar amount of cement, however did not achieve the compressive strength of S10-48L. Creep results from S10-48L are shown with mix Nos. 9-12 in **Figure 3.9**. All specimens tested in Long and Khayat (2011) were loaded to 40% of their measured compressive strength, but at 18 hours age. The lower creep strain experienced

by the specimens in this study relative to Long and Khayat are possibly due to the concrete in the study being loaded at a later age when the strength and stiffness has increased relative to that of 18 hour old concrete.

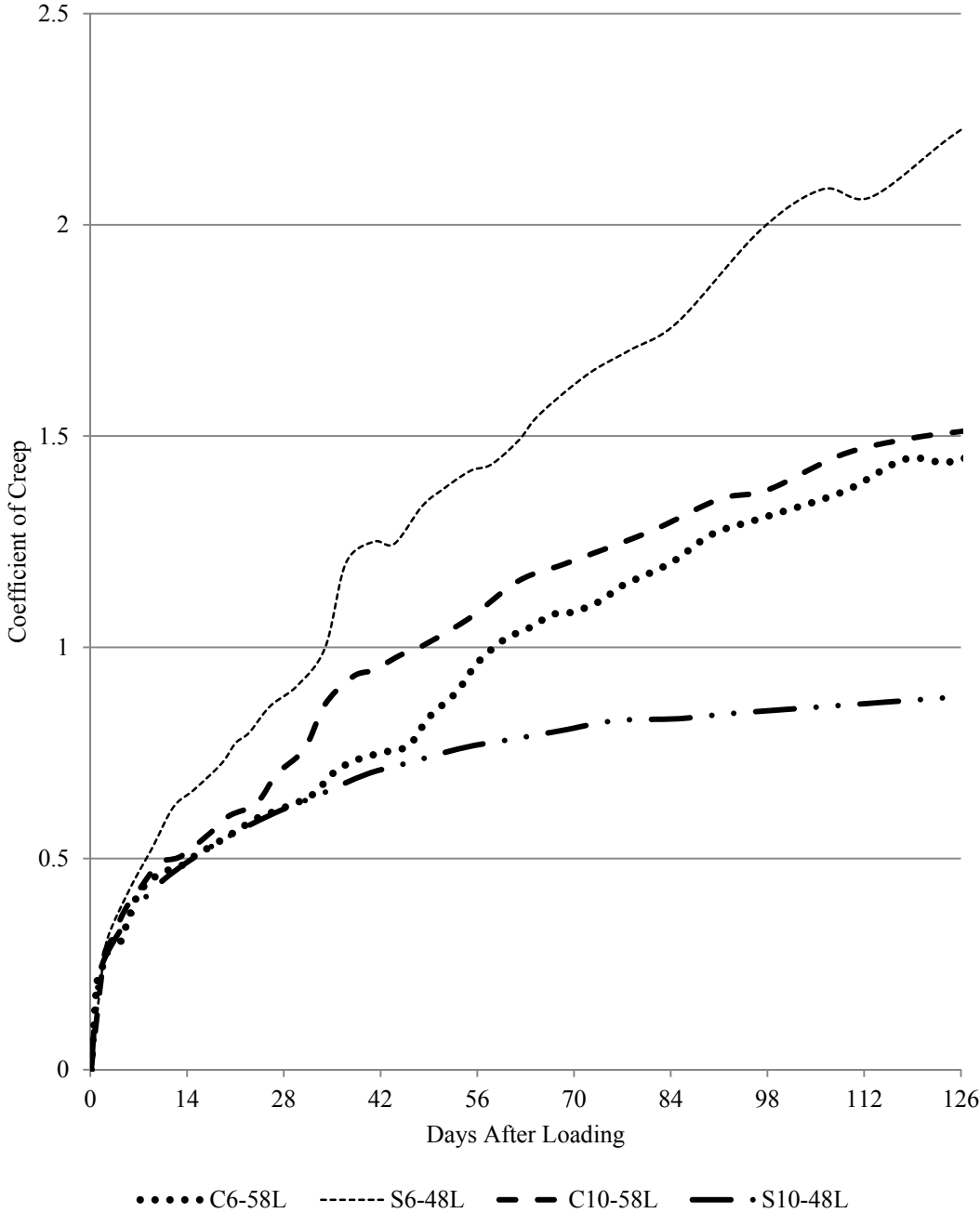


Figure 3.7 – SCC Coefficient of Creep Results

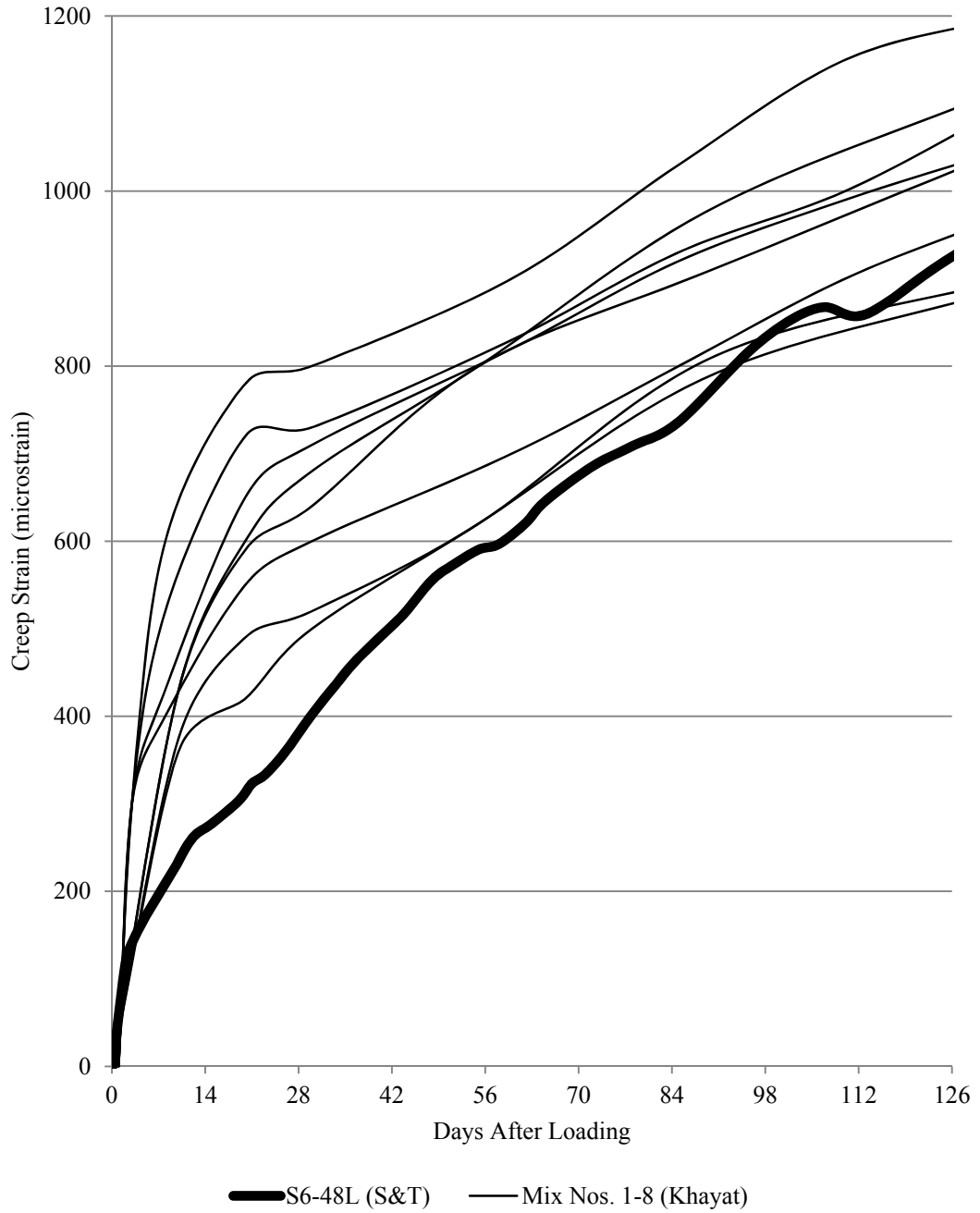


Figure 3.8 – S6-48L Plotted Against Results from Long and Khayat (2011)

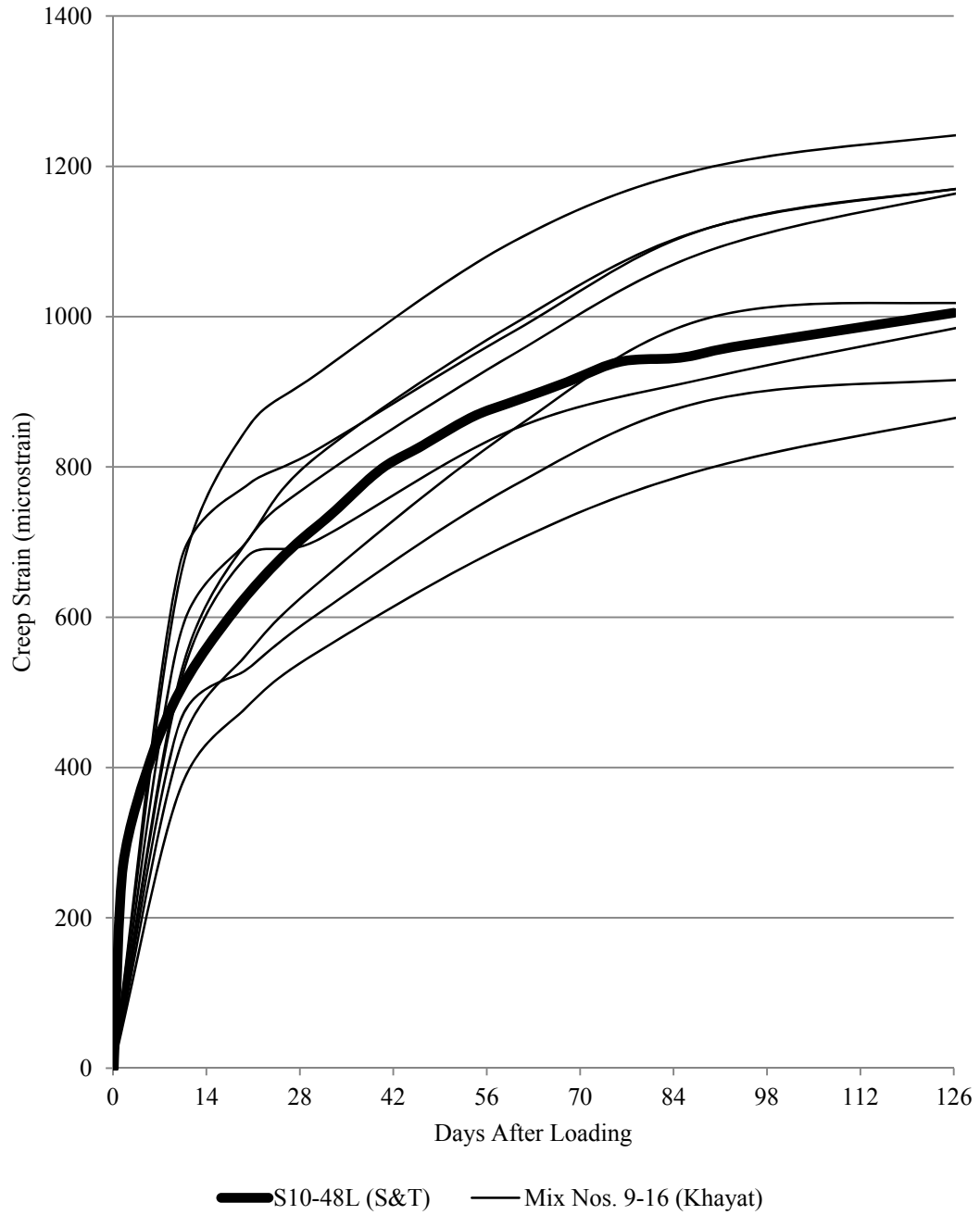


Figure 3.9 – S10-48L Plotted Against Results from Long and Khayat (2011)

3.3. ABRASION RESISTANCE

3.3.1. Results. Figures 3.10 – 3.13 show the mass losses recorded after each two minute abrasion cycle for each mix tested. Figure 3.14 shows the cumulative mass loss comparison between the four mixes. Figure 3.15 shows the depth of wear results from abrasion testing. Table 3.3 shows a summary of all results along with measured 28 day compressive strength. One test consisted of three cycles.

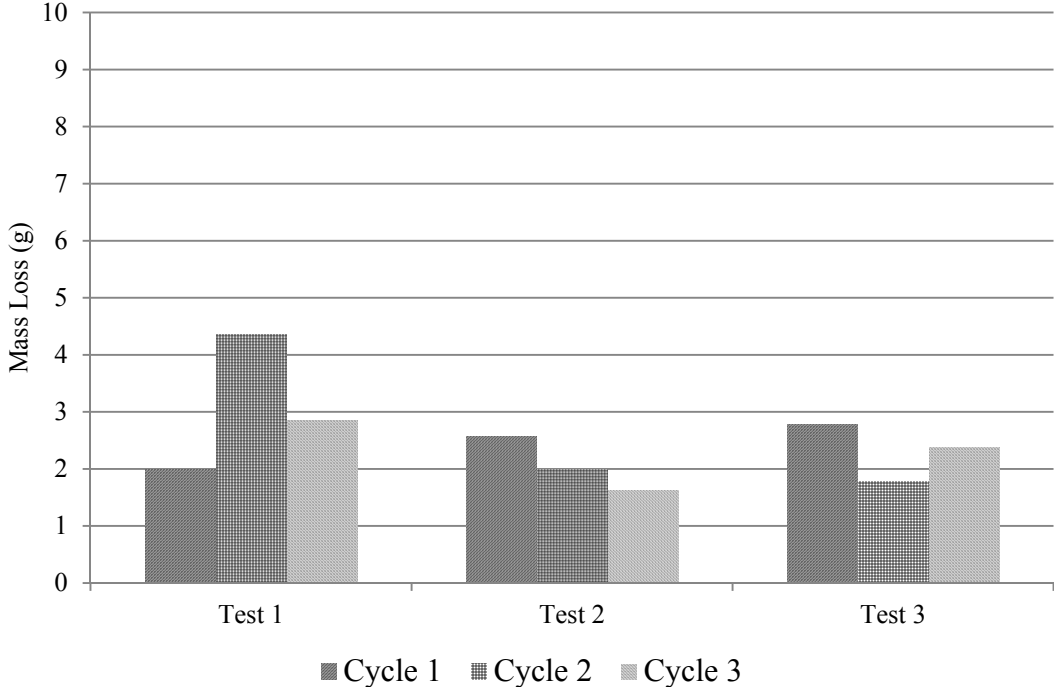


Figure 3.10 - C6-58L Mass Loss Results

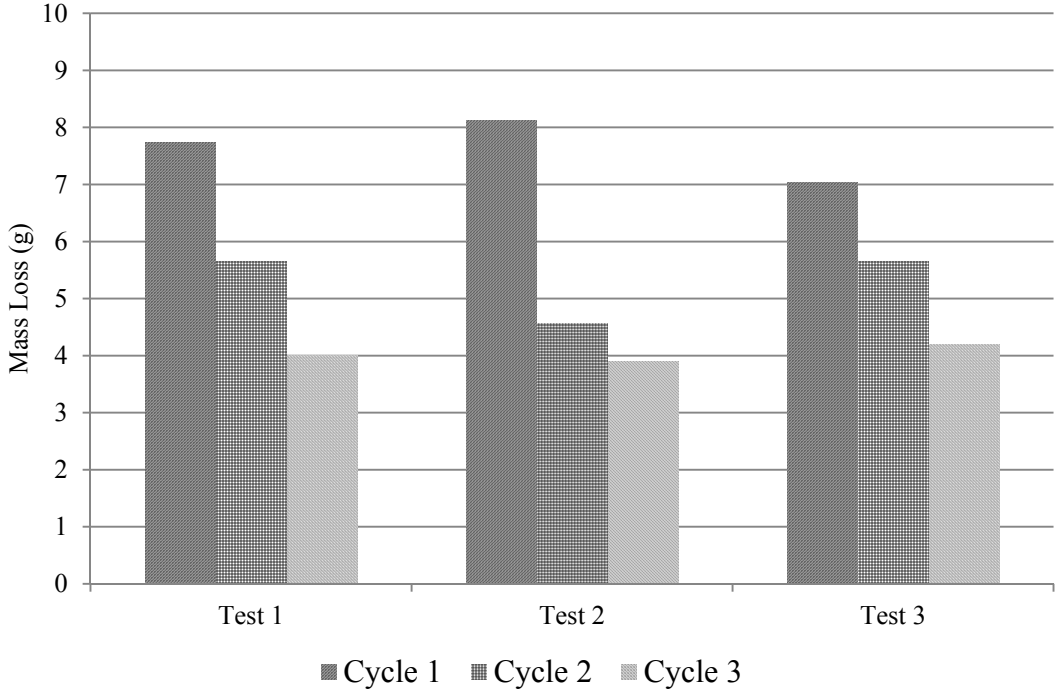


Figure 3.11 - S6-48L Mass Loss Results

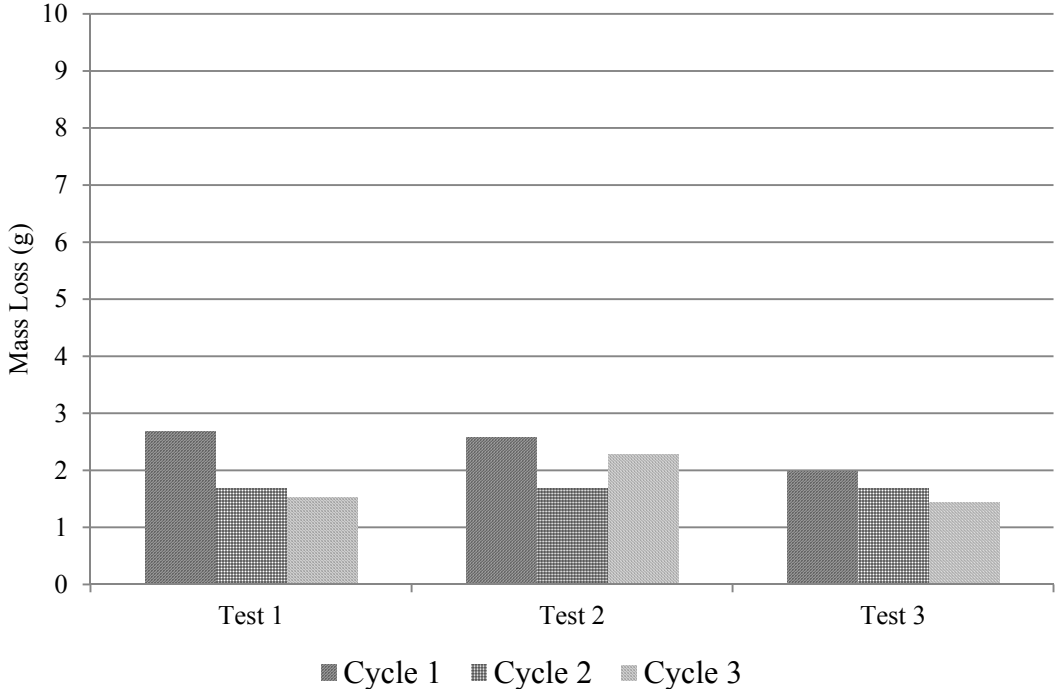


Figure 3.12 - C10-58L Mass Loss Results

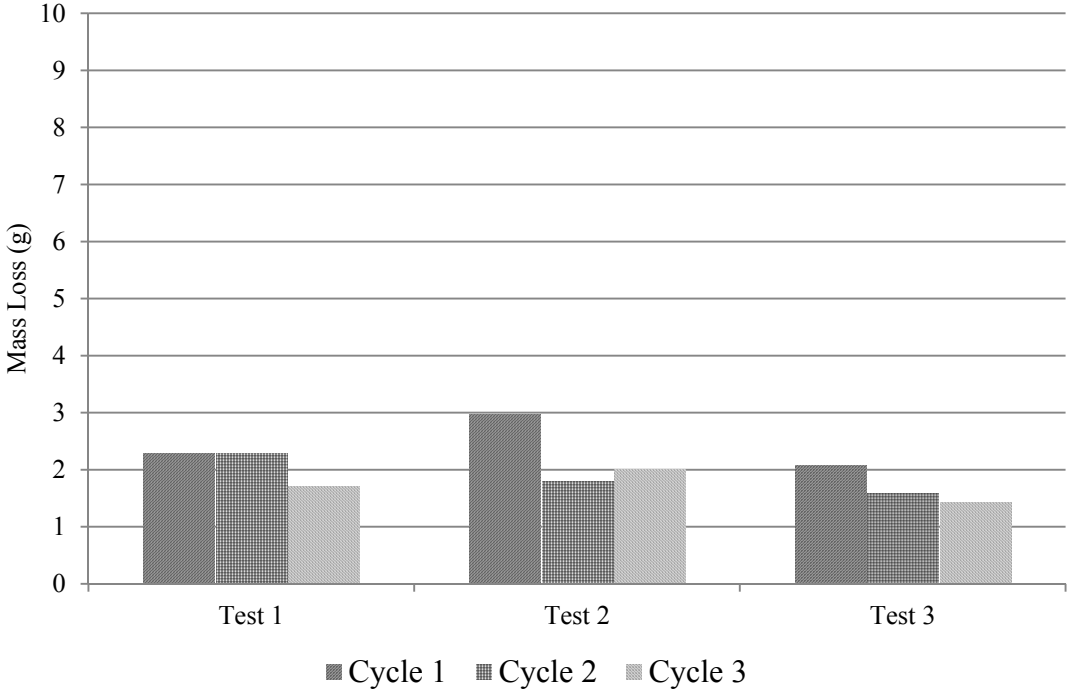


Figure 3.13 - S10-48L Mass Loss Results

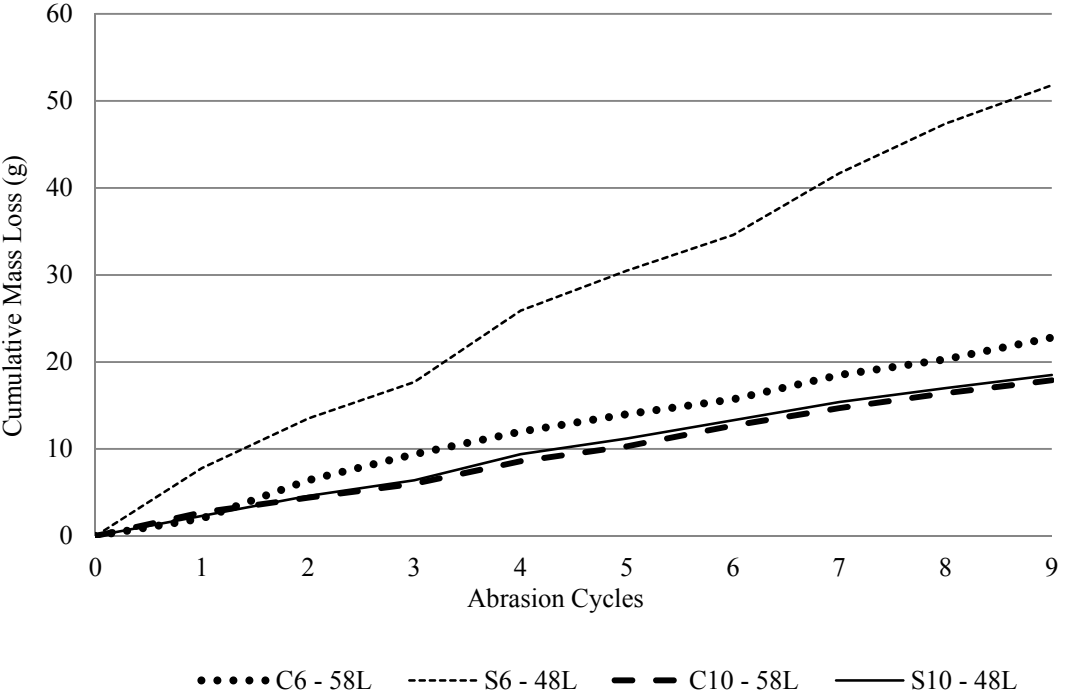


Figure 3.14 - SCC Mass Loss Results

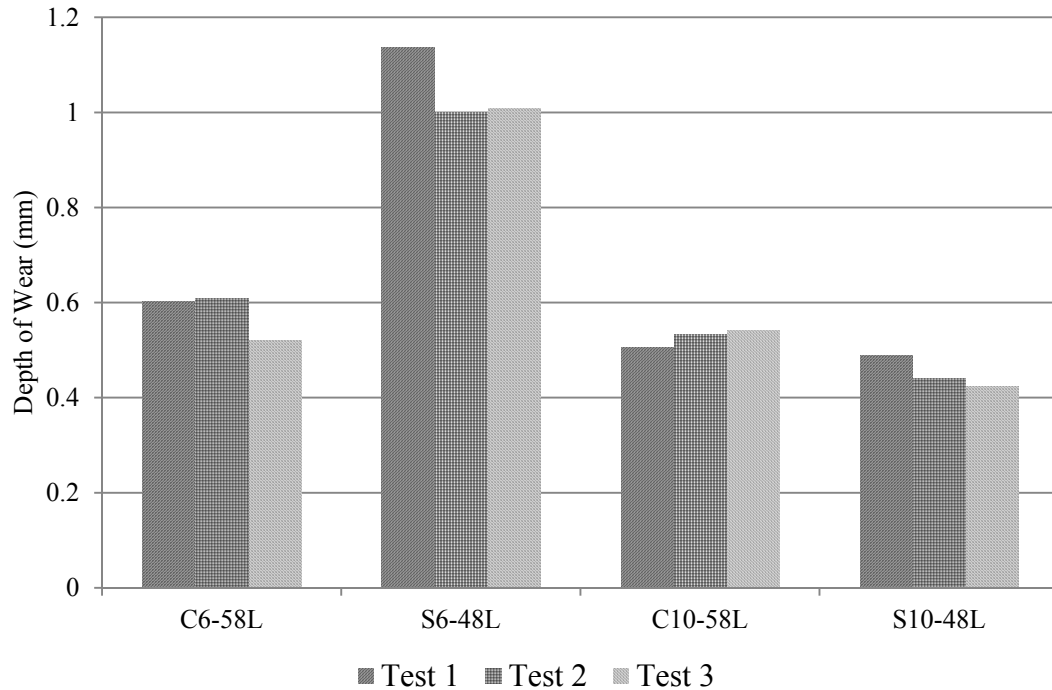


Figure 3.15 - SCC Depth of Wear Results

Table 3.3 - Summary of Results Shown with 28 Day Measured Compressive Strength

	C6-58L	S6-48L	C10-58L	S10-48L
28 Day Compressive Strength (psi)	7,000	5,500	11,000	13,500
Avg. Mass loss (g)	2.53	5.76	1.99	2.06
Avg. Depth of Wear (mm)	0.59	1.07	0.54	0.47

Conversion: 1 MPa = 145.04 psi

1 lb. = 453.59 g

1 in. = 25.4 mm

3.3.2. Discussion and Conclusions. The results obtained are very consistent with trends found in previous studies. As was concluded in both Atis and Naik, the abrasion resistance of concrete is primarily dependent on compressive strength. For both

criteria (mass loss and depth of abrasion), the abrasion resistance of concrete increased as the compressive strength of the specimens increased, except for the mass loss of S10-48L relative to C10-58L. Additionally, when comparing concrete mixes with the same design strength, the SCC mix generally showed a lower resistance to wear. This is most likely due to the decreased amount of coarse aggregate in the SCC mixes. Based on observations during and after testing, the majority of mass loss due to abrasion was from the cement paste, as opposed to the aggregate. Generally, for each test, cycle 1 shows the greatest amount of mass loss. The general decrease in measured mass loss for each subsequent cycle indicates that as the depth of wear gets larger, the presence of aggregate begins to take effect. This would explain why the SCC mixes showed a decrease in abrasion resistance relative to their conventional concrete equivalents.

APPENDIX A.
SHRINKAGE DATA WITH RELATIVE HUMIDITY DATA

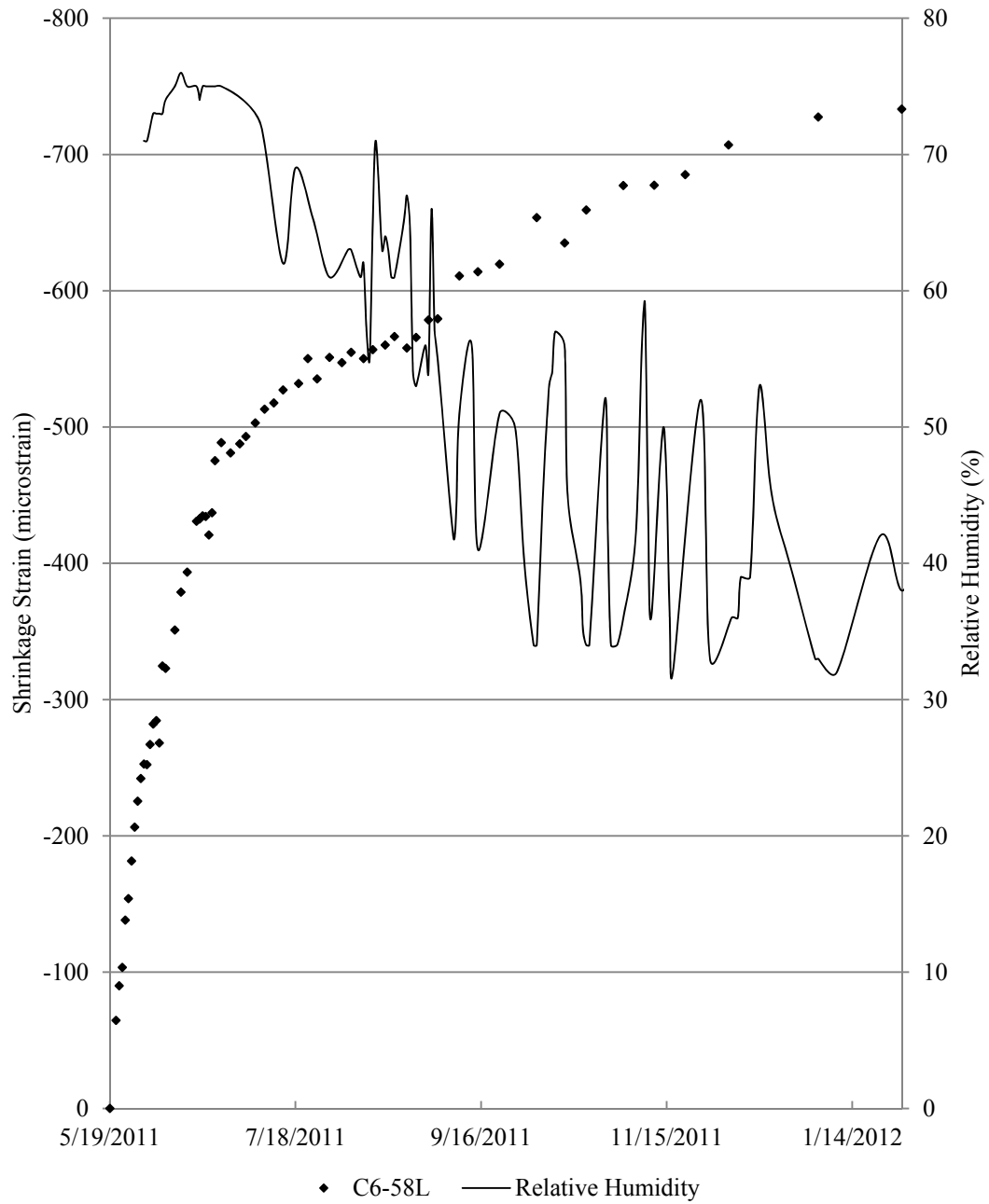


Figure A.1 – C6-58L shrinkage data shown with recorded relative humidity

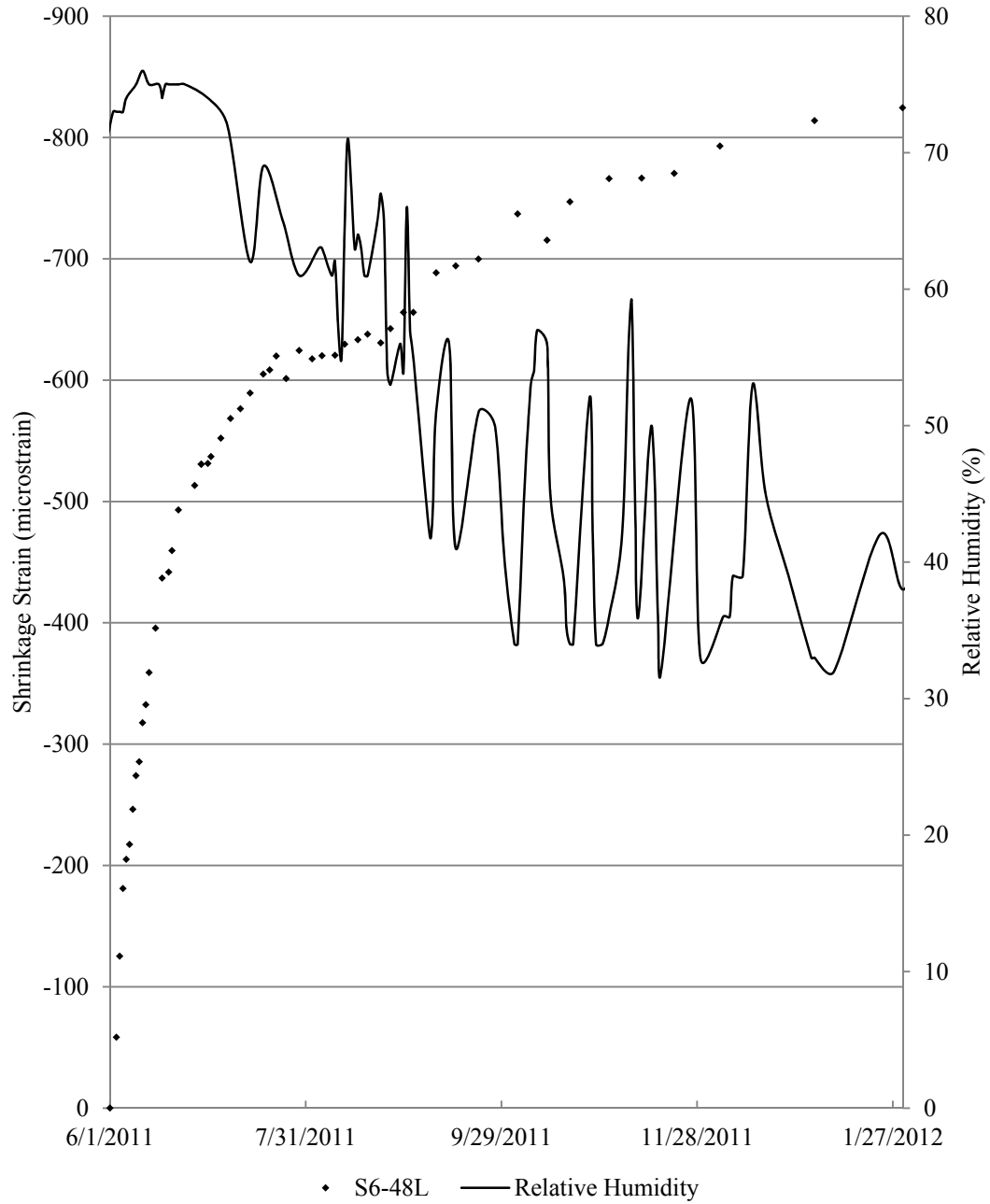


Figure A.2 - S6-48L shrinkage data shown with recorded relative humidity

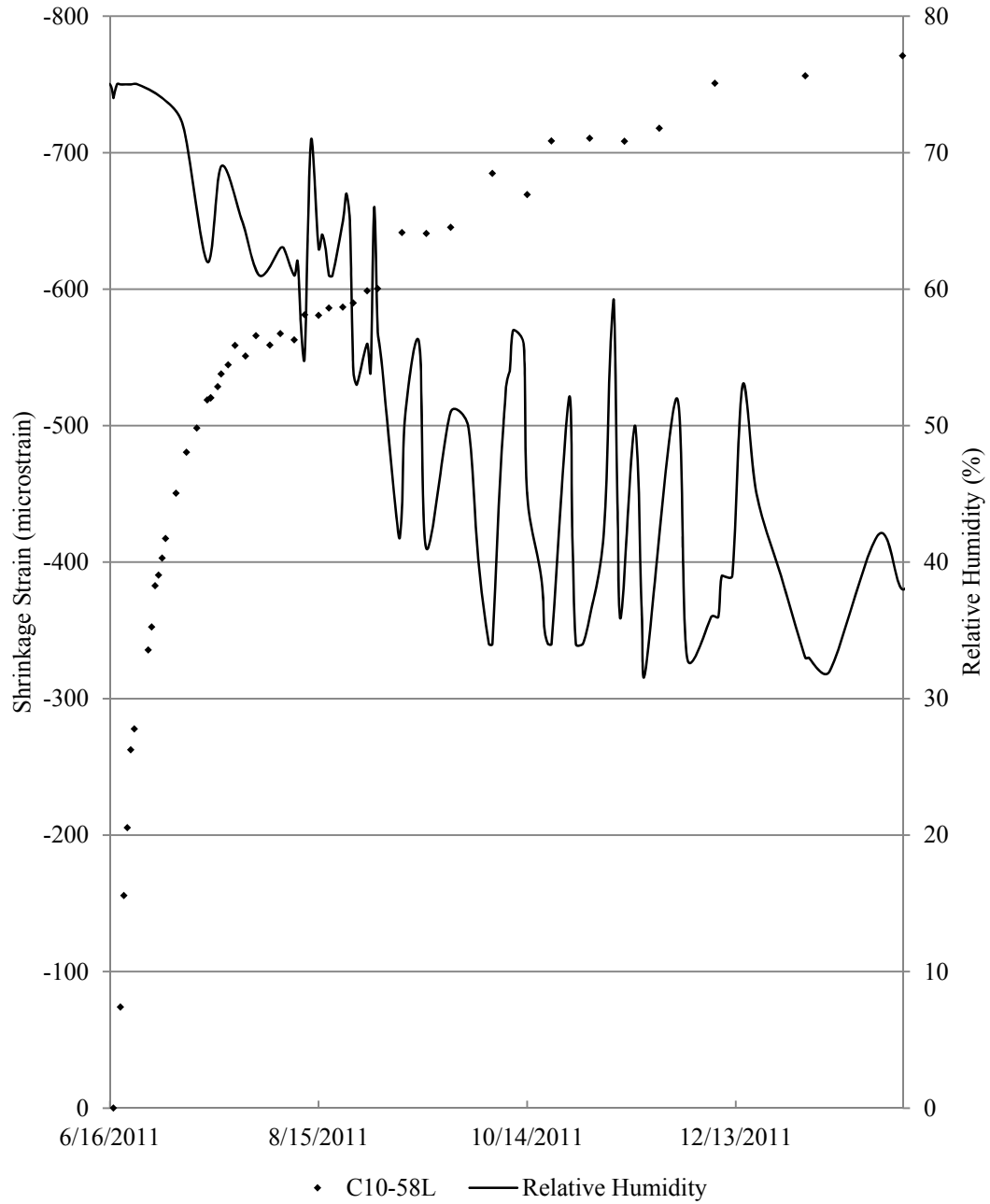


Figure A.3 – C10-58L shrinkage data shown with recorded relative humidity

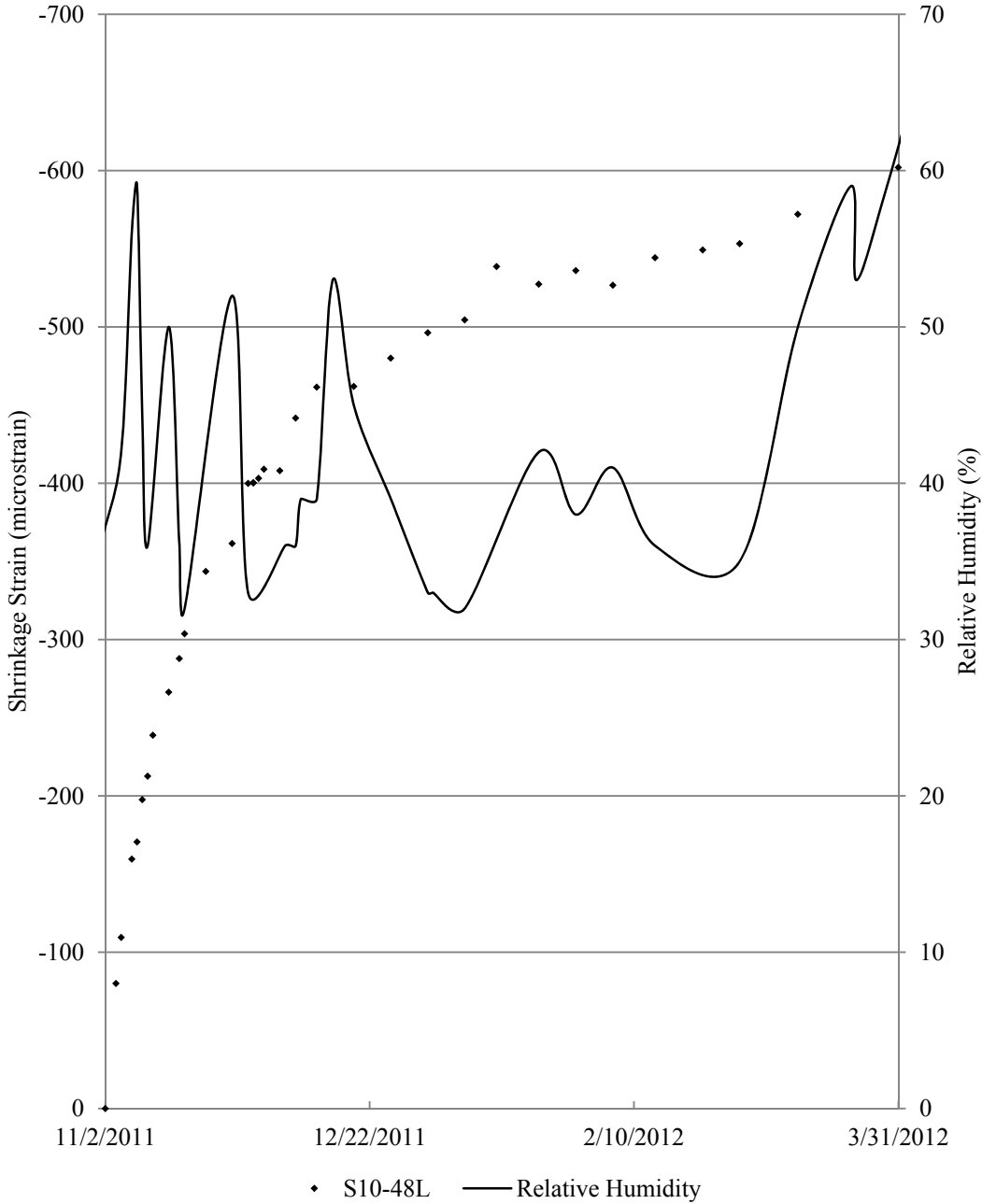


Figure A.4 – S10-48L shrinkage data shown with recorded relative humidity

APPENDIX B.
EXAMPLE STRAIN CALCULATIONS

	A	B	C	D	E	F	G
1			Example Shrinkage and Creep Calculation				
2							
3			G= 0.40 x 10 ⁻⁵ (mm/mm)				
4			G= 4.00 x 10 ⁻⁶ (mm/mm)				
5							
6					Measured Data		
7			Specimen	Reading			
8			Refer Bar		2525	2524	2525
9			C6-58L SH1	1--1	2130	2111	2106
10			C6-58L SH1	1--2	3633	3615	3611
11			C6-58L SH1	1--3	4018	4002	3998
12			C6-58L SH1	2--1	2549	2531	2529
13			C6-58L SH1	2--2	3179	3162	3162
14			C6-58L SH1	2--3	3230	3213	3210
15			C6-58L SH1	3--1	5867	5846	5846
16			C6-58L SH1	3--2	1980	1962	1960
17			C6-58L SH1	3--3	2182	2166	2165
18							
19							
20					Calculated Strain		
21							
22			C6-58L SH1	1--1		-72	-24
23			C6-58L SH1	1--2		-68	-20
24			C6-58L SH1	1--3		-60	-20
25			C6-58L SH1	2--1		-68	-12
26			C6-58L SH1	2--2		-64	-4
27			C6-58L SH1	2--3		-64	-16
28			C6-58L SH1	3--1		-80	-4
29			C6-58L SH1	3--2		-68	-12
30			C6-58L SH1	3--3		-60	-8
31							
32			Average Shrinkage			-67.1	-13.3
33			Cumulative Shrinkage			-67.1	-80.4
34							

Figure B.1 – Example shrinkage and creep strain calculation

	A	B	C	D	E	F	G
1			Example Shrinkage and Creep Calculation				
2							
3			G= 0.4 x 10 ⁻⁵ (mm/mm)				
4			G= 4 x 10 ⁻⁶ (mm/mm)				
5							
6						Measured Data	
7			Specimen	Reading			
8			Refer Bar		2525	2524	2525
9			C6-58L SH1	1--1	2130	2111	2106
10			C6-58L SH1	1--2	3633	3615	3611
11			C6-58L SH1	1--3	4018	4002	3998
12			C6-58L SH1	2--1	2549	2531	2529
13			C6-58L SH1	2--2	3179	3162	3162
14			C6-58L SH1	2--3	3230	3213	3210
15			C6-58L SH1	3--1	5867	5846	5846
16			C6-58L SH1	3--2	1980	1962	1960
17			C6-58L SH1	3--3	2182	2166	2165
18							
19							
20						Calculated Strain	
21							
22			C6-58L SH1	1--1		=B5*(F9-E9)-(F8-E8))	=B5*(G9-F9)-(G8-F8))
23			C6-58L SH1	1--2		=B5*(F10-E10)-(F8-E8))	=B5*(G10-F10)-(G8-F8))
24			C6-58L SH1	1--3		=B5*(F11-E11)-(F8-E8))	=B5*(G11-F11)-(G8-F8))
25			C6-58L SH1	2--1		=B5*(F12-E12)-(F8-E8))	=B5*(G12-F12)-(G8-F8))
26			C6-58L SH1	2--2		=B5*(F13-E13)-(F8-E8))	=B5*(G13-F13)-(G8-F8))
27			C6-58L SH1	2--3		=B5*(F14-E14)-(F8-E8))	=B5*(G14-F14)-(G8-F8))
28			C6-58L SH1	3--1		=B5*(F15-E15)-(F8-E8))	=B5*(G15-F15)-(G8-F8))
29			C6-58L SH1	3--2		=B5*(F16-E16)-(F8-E8))	=B5*(G16-F16)-(G8-F8))
30			C6-58L SH1	3--3		=B5*(F17-E17)-(F8-E8))	=B5*(G17-F17)-(G8-F8))
31							
32			Average Shrinkage			=AVERAGE(F22:F30)	=AVERAGE(G22:G30)
33			Cumulative Shrinkage			=F32	=F33+G32
34							
35							

Figure B.2 – Example shrinkage and creep strain calculations with equations shown

APPENDIX C.
COEFFICIENT OF VARIATION DATA

C6-58L		Shrinkage														
Age (days)		2	3	4	5	6	7	8	9	10	11	12	13	14	15	16
COV		0.20	0.62	0.46	0.25	0.74	0.41	0.25	0.62	0.42	0.45	9.57	0.28	0.25	7.83	1.21
		17	18	21	23	25	28	29	30	31	32	33	34	36	39	42
		0.25	6.75	0.27	0.19	0.36	0.17	1.94	1.11	5.25	0.82	0.72	0.18	0.53	1.38	0.58
		44	47	50	53	56	61	64	67	71	75	78	82	85	89	92
		0.51	0.59	0.28	0.53	0.38	0.61	0.17	0.22	0.20	0.57	0.31	0.53	0.41	0.62	0.55
		96	99	103	106	113	119	126	138	147	154					
		0.28	0.37	0.25	2.91	0.18	0.94	0.56	0.16	0.43	0.38					
		Creep														
Age (days after loading)					1	2	3	4	5	7	10	13	15	18	21	24
COV					0.60	0.55	0.89	0.87	0.21	0.48	1.04	0.46	0.43	0.40	0.39	0.43
		27	32	35	38	42	46	49	53	56	60	63	67	70	74	77
		0.32	0.45	0.22	3.68	1.22	3.35	0.33	1.37	0.63	0.62	0.46	1.02	0.45	0.34	0.54
		84	90	97	109	118	125									
		0.35	0.51	0.48	0.34	3.29	0.37									
		S6-48L														
		Shrinkage														
Age (days)		2	3	4	5	6	7	8	9	10	11	12	14	16	18	19
COV		0.50	0.45	0.31	0.48	0.74	0.21	0.16	0.65	0.24	0.24	0.13	0.16	0.10	0.51	0.37
		21	26	28	30	31	34	37	40	43	47	49	51	54	58	62
		0.26	0.31	0.21	3.74	0.36	0.18	0.18	0.48	0.18	0.21	1.01	0.27	0.20	0.14	0.42
		65	69	72	76	79	83	86	90	93	100	106	113	125	134	141
		0.77	6.64	0.40	0.66	0.58	0.32	0.31	0.19	0.00	0.17	0.53	0.90	0.17	0.16	0.16
		153														
		0.17														
		Creep														
Age (days after loading)					2	3	6	9	12	15	19	21	23	26	30	34
COV					0.92	0.21	0.18	0.17	0.22	0.15	0.13	0.43	0.62	2.29	0.11	1.66
		37	41	44	48	51	55	58	62	65	72	78	85	97	106	113
		0.41	0.42	1.56	1.03	0.89	2.71	0.47	0.54	0.85	0.42	0.56	0.52	0.95	3.30	0.35
		125														
		0.31														

Figure C.1 – C6-58L and S6-48L COV Data

C10-58L		Shrinkage														
Age (days)		2	3	4	5	6	10	11	12	13	14	15	18	21	24	27
COV		0.08	0.16	0.26	0.18	0.42	0.13	0.18	0.12	0.87	0.56	0.19	0.12	0.12	0.17	0.15
		28	30	31	33	35	38	41	45	48	52	55	59	62	66	69
		1.41	0.39	0.33	0.46	0.22	0.65	0.20	0.27	0.32	0.53	0.15	5.25	0.36	3.09	1.13
		73	76	83	90	97	109	119	126	137	147	157				
		0.40	1.56	0.16	3.09	0.61	0.11	0.21	0.10	1.24	0.92	0.25				
		Creep														
Age (days after loading)					2	3	5	7	10	13	17	20	24	27	31	34
COV					1.73	0.34	0.34	0.38	0.55	0.42	0.40	0.20	0.34	0.16	0.70	9.37
		38	41	45	48	55	62	69	81	91	98	109	119	129		
		1.89	0.49	0.21	0.62	0.17	0.29	0.21	0.17	0.58	0.14	0.27	0.20	0.14		
		S10-48L														
		Shrinkage														
Age (days)		2	3	5	6	7	8	9	12	14	15	19	24	27	28	29
COV		0.10	0.18	0.08	0.26	0.15	0.27	0.15	0.14	0.20	0.28	0.10	0.18	0.11	8.19	1.30
		30	33	36	40	47	54	61	68	74	82	89	96	104	113	120
		0.42	18.62	0.48	0.13	5.92	0.16	0.20	0.32	0.11	0.26	0.33	0.40	0.30	0.46	0.35
		131														
		0.87														
		Creep														
Age (days after loading)					1	2	5	8	12	19	26	33	40	46	54	61
COV					0.27	0.19	0.16	0.15	0.16	0.17	0.13	0.15	0.14	0.15	0.29	0.18
		68	76	85	92	103	126									
		0.4	0.18	9.27	0.22	0.13	0.45									

Figure C.2 – C10-58L and S10-48L COV Data

BIBLIOGRAPHY

- American Concrete Institute (ACI 116R-00) (2000), "Cement and Concrete Terminology." American Concrete Institute, Detroit, Michigan.
- American Concrete Institute (ACI 209R-92) (1997), "Prediction of Creep, Shrinkage, and Temperature Effects in Concrete Structures." American Concrete Institute, Detroit, Michigan.
- American Concrete Institute (ACI 209.1R-05) (2005), "Report on Factors Affecting Shrinkage and Creep of Hardened Concrete." American Concrete Institute, Detroit, Michigan.
- American Concrete Institute (ACI 237R-07) (2007), "Self-Consolidating Concrete." American Concrete Institute, Detroit, Michigan.
- American Concrete Institute (ACI 318-08) (2008), "Building Code Requirements for Structural Concrete and Commentary." American Concrete Institute, Detroit, Michigan.
- ASTM C31/C31 M-09 (2009). "Standard Practice for Making and Curing Concrete Test Specimens in the Field." American Society for Testing and Materials, West Conshohocken, Pennsylvania.
- ASTM C39/C39 M-05 (2005). "Standard Test Method for Compressive Strength of Cylindrical Concrete Specimens." American Society for Testing and Materials, West Conshohocken, Pennsylvania.
- ASTM C157/C157 M-08 (2008). "Standard Practice for Length Change of Hardened Hydraulic-Cement Mortar and Concrete." American Society for Testing and Materials, West Conshohocken, Pennsylvania.
- ASTM C3512/C512 M-10 (2010). "Standard Practice for Creep of Concrete in Compression." American Society for Testing and Materials, West Conshohocken, Pennsylvania.
- ASTM C944/C944 M-99 (2005). "Standard Practice for Abrasion Resistance of Concrete of Mortar Surfaces by the Rotating-Cutter Method." American Society for Testing and Materials, West Conshohocken, Pennsylvania.

- Bazant, Z. P. and Baweja, S. (2000). "Creep and Shrinkage Prediction Model for Analysis and Design of Concrete Structures: Model B3" Adam Neville Symposium: Creep and Shrinkage—Structural Design Effects, ACI SP-194, A. Al-Manaseer, ed., Am. Concrete Institute, Farmington Hills, Michigan, 2000, 1–83.
- Branson, D. E., and Christiason, M. L. (1971) "Time-Dependent Concrete Properties Related to Design-Strength and Elastic Properties," Designing for Effects of Creep, Shrinkage, Temperature in Concrete Structures, SP-27, American Concrete Institute, Detroit, MI, pp. 257-277.
- Comite Euro – International Du Beton (CEB) (1990), "CEB-FIP Model Code 1990" Thomas Telford, 1990-1993, 53-58.
- Fernandez-Gomez, J. and Landsberger, G.A. (2007). "Evaluation of Shrinkage Prediction Models for Self-Consolidating Concrete." ACI Materials Journal, October 2007, 464-473.
- Freyermuth, C.L. (1969). "Design of Continuous Highway Bridges with Precast, Prestressed Concrete Girders." Journal of the Prestressed Concrete Institute, Vol. 14, No. 2, 14-39.
- Gardner, N.J., and Lockman, M.J. (2001), "Design Provisions for Drying Shrinkage and Creep of Normal-Strength Concrete" ACI Materials Journal, 159-167.
- Holschemacher, K (2004). "Hardened Material Properties of Self-Compacting Concrete" Journal of Civil Engineering and Management, Vol X, No 4, 261-266.
- Khayat, K.H., and Mitchell, D. (2009). "Self-Consolidating Concrete for Precast, Prestressed Concrete Bridge Elements." National Cooperative Highway Research Program Report 628, Transportation Research Board, Washington, D.C.
- Long, W., Khayat, K.H., and Xing, F. (2011). "Autogenous Shrinkage of Prestressed Self-Consolidating Concrete." The Open Civil Engineering Journal, 2011, 5, 116-123.
- Long, et. al. (2011). "Statistical Models to Predict Fresh and Hardened Properties of Self-Consolidating Concrete." RILEM Materials and Structures, 2001.
- Myers, J.J., Carrasquillo, R.L. (1999). "The Production and Quality Control of High Performance Concrete in Texas Bridge Structures," Center for Transportation Research, Report Number 580-589-1, November 1999, pp 564.
- Myers, J.J. and Yang, Y. (2004). "High Performance Concrete for Bridge A6130-Route 412 Pemiscot County, MO," Missouri Department of Transportation, Report RDT 04-016, June 2004.

- Perenchio, W.F., (1997). "The Drying Shrinkage Dilemma-Some Observations and Questions About Drying Shrinkage and its Consequence," *Concrete Construction*, V. 42, No. 4, pp. 379-383.
- Schindler, A.K., et. al. (2007). "Properties of Self-Consolidating Concrete for Prestressed Members." *ACI Materials Journal*, January-February 2007, 53-61.
- Tadros, M.K., Al-Omaishi, N., Seguirant, S.J., and Gallt, J.G. (2003). "Prestress Losses in Pretensioned High-Strength Concrete Bridge Girders." National Cooperative Highway Research Program Report 496, Transportation Research Board, National Research Council, Washington, D.C.